Synthesis, Structure, and Reactivity of Zerovalent Group 6 Metal Pentacarbonyl Aryl Oxide Complexes. Reactions with Carbon Dioxide

Donald J. Darensbourg,*[1a] Kathryn M. Sanchez,[1a] Joseph H. Reibenspies,[1a] and Arnold L. Rheingold[1b]

Contribution from the Departments of Chemistry, Texas A&M University, College Station, Texas 77843, and University of Delaware, Newark, Delaware 19716.
Received February 22, 1989

Abstract: The synthesis of $[Et_4N][M(CO)_5OR]$ (M = Cr, Mo, W; R = Ph, $C_6H_4CH_3$-*m*) from the reaction of $M(CO)_5THF$ and $[Et_4N][OR]$ in tetrahydrofuran is reported. In the absence of a carbon monoxide atmosphere these mononuclear species readily aggregate via a CO dissociation pathway to the tetranuclear species $[Et_4N]_4[M(CO)_3OR]_4$. It was possible to isolate pure crystalline samples of the $[Et_4N][W(CO)_5OR]$ derivatives by precipitation from solutions under a carbon monoxide atmosphere. The $[Et_4N][W(CO)_5OPh]$ complex was characterized in the solid-state by X-ray crystallography. $[Et_4N][W(CO)_5OPh]$ crystallizes in the space group $P\bar{1}$ with cell dimensions a = 9.416 (3) Å, b = 12.665 (2) Å, c = 18.371 (3) Å, α = 92.38 (1)°, β = 94.50 (2)°, γ = 95.85 (2)°, V = 2168.3 Å^3, Z = 4, and R_F = 7.71%. An additional salt of the tungsten phenoxide complex has been crystallized that contains 0.5 equiv of water, i.e., $[Et_4N][W(CO)_5OPh\cdot 0.5H_2O]$. This species has as well been characterized by X-ray crystallography. $[Et_4N][W(CO)_5OPh\cdot 0.5H_2O]$ crystallizes in the space group $P2_1/c$ with cell dimensions a = 17.545 (5), b = 25.322 (8), c = 10.337 (3), β = 102.52 (3)°, V = 4483 (2) Å^3, Z = 8, and R_F = 5.60%. The water molecule is shown to be hydrogen bonded between ligated –OPh ligands of adjacent $W(CO)_5OPh^-$ anions. This intermolecular hydrogen-bonding interaction is observed in tetrahydrofuran solution as well between alcohols and $W(CO)_5OPh^-$. The $M(CO)_5OR^-$ (M = Cr, W) derivatives were demonstrated to undergo facile insertion reactions with CO_2, COS, and CS_2 to afford the corresponding metal pentacarbonyl phenyl carbonate, phenyl thiocarbonate, and phenyl dithiocarbonate complexes. This carbon dioxide insertion reaction is reversible, and the rate of insertion is unaffected by carbon monoxide pressures up to 10 atm. The relative rates of insertion of CO_2, COS, and CS_2 into the $M(CO)_5OPh^-$ anions are Cr > W and CS_2 > COS > CO_2. On the other hand, in the presence of ligands at the metal center that are sterically more demanding than CO, i.e., *cis*-$M(CO)_4(L)OPh^-$ derivatives, the relative rates of carbon dioxide insertion are W > Cr and L = $P(OMe)_3$ > PMe_3 > PPh_3. The $W(CO)_5XC(X)OPh^-$ (X = O or S) derivatives underwent hydrolysis in the presence of small quantities of water to provide the corresponding $W(CO)_4(CX_2O)^{2-}$ products. One of these products, namely, $[Et_4N]_2[W(CO)_4CO_3]$, was subjected to an X-ray crystallographic investigation. The salt crystallizes in the $P\bar{1}$ space group with cell dimensions a = 10.513 (5) Å, b = 15.881 (10) Å, c = 8.130 (6) Å, α = 101.69 (6)°, β = 92.12 (5)°, γ = 83.25 (5)°, V = 1319.8 Å^3, Z = 2, and R_F = 3.01%. The W–O bond distances (2.204 Å) are quite similar to those observed (2.203 Å) in the W–OPh^- complexes. The carbonate ligand is bidentate with a very acute O–W–O angles of 59.4°.

The intermediacy of low-valent group 6 transition-metal alkoxide complexes in catalytic processes has been established. These include the hydrogenation of ketones and aldehydes with anionic metal hydrides, $HM(CO)_5^-$ and *cis*-$HM(CO)_4P(OMe)_3^-$ (M = Cr, W),[2] where the pivotal step is indicated in eq 1 with subsequent

$$[M]H^- + R_2O \rightleftharpoons [M]OCHR_2^- \qquad (1)$$

quenching of the metal–alkoxide intermediate with a Brønsted acid leading to production of the corresonding alcohol. This reaction has been made catalytic with $M(CO)_5B^-$ (M = Cr, W; B = Brønsted base)[3] or $HCr_2(CO)_{10}^{4-}$ in the presence of hydrogen pressure. A proposed cycle for the catalytic reduction of aldehydes and ketones is indicated in Scheme I.

Tentative identification of a metal alkoxide complex in the reduction process has been reported for the reactions of $HCr(CO)_5^-$ with paraformaldehyde and *cis*-$HW(CO)_4P(OMe)_3^-$ with paraformaldehyde, propionaldehyde, or benzaldehyde.[2] However, the isolation of a metal alkoxide complex from these reactions has not been possible.

The tungsten hexacarbonyl/potassium methoxide catalyzed carbonylation of methanol to produce methyl formate may also involve a metal alkoxide complex as an intermediate.[5,6] The formation of the key intermediate, a tungsten methoxycarbonyl

Scheme I

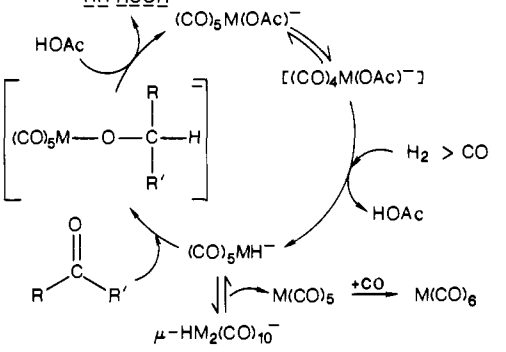

complex, $W(CO)_5C(O)OCH_3^-$, may proceed via either of two pathways (eq 2 and 3). There is ample precedent in the literature

$$W(CO)_6 + OCH_3^- \rightleftharpoons W(CO)_5C(O)OCH_3^- \qquad (2)$$

$$W(CO)_5OCH_3^- + CO \rightleftharpoons W(CO)_5C(O)OCH_3^- \qquad (3)$$

for both routes in other transition-metal systems.[7,8] In eq 2, nucleophilic attack by free methoxide ion on a coordinated car-

(1) (a) Texas A&M University. (b) University of Delaware.
(2) Gaus, P. L.; Kao, S. C.; Youngdahl, K.; Darensbourg, M. Y. *J. Am. Chem. Soc.* **1985**, *107*, 2428.
(3) Tooley, P. A.; Ovalles, C.; Kao, S. C.; Darensbourg, D. J.; Darensbourg, M. Y. *J. Am. Chem. Soc.* **1986**, *108*, 5465.
(4) Marko, L.; Nagy-Magos, Z. *J. Organomet. Chem.* **1985**, *285*, 193.
(5) Darensbourg, D. J.; Gray, R. L.; Ovalles, C.; Pala, M. *J. Mol. Catal.* **1985**, *29*, 285.
(6) Darensbourg, D. J.; Gray, R. L.; Ovalles, C. *J. Mol. Catal.* **1987**, *41*, 329.
(7) (a) Bryndza, H. E.; Calabrese, J. C.; Wreford, S. S. *Organometallics* **1984**, *3*, 1603. (b) Bryndza, H. E.; Kretchman, S. A.; Tulip, T. H. *J. Chem. Soc., Chem. Commun.* **1985**, 977. (c) Bryndza, H. E. *Organometallics* **1985**, *4*, 1686.
(8) (a) Rees, W. M.; Churchill, M. R.; Fettinger, J. C.; Atwood, J. D. *Organometallics* **1985**, *4*, 2179. (b) Rees, W. M.; Atwood, J. D. *Organometallics* **1985**, *4*, 402. (c) Churchill, M. R.; Fettinger, J. C.; Rees, W. M; Atwood, J. D. *J. Organomet. Chem.* **1986**, *308*, 361.

0002-7863/89/1511-7094$01.50/0

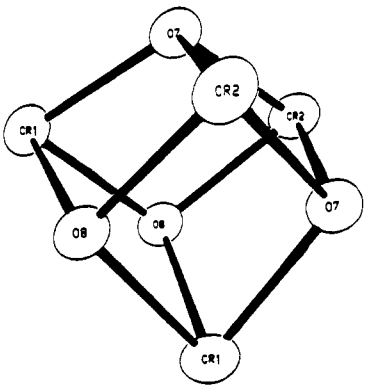

Figure 1. Structure of the Cr_4O_4 core in the $[Cr_4(CO)_{12}(\mu\text{-}OR)_4]^{4-}$ anion, where R = H and CH_3, taken from ref 18.

bonyl ligand forms the methoxycarbonyl moiety, whereas, the alternative pathway entails migratory insertion of carbon monoxide into the tungsten–methoxide bond. In protic solvents the former process has been established.[6,9]

Several laboratories have reported on the formation and isolation of binuclear and polynuclear low-valent group 6 metal carbonyl complexes containing bridging alkoxide and hydroxide ligands. The earliest studies were reported by Hieber and co-workers,[10-13] where the reaction of $M(CO)_6$ (M = Cr, Mo, W) with hydroxide ion in methanol afforded $K_3[M_2(CO)_6(OR)_3]$ (M = Cr, Mo, W; R = H, CH_3). $K_3[W_2(CO)_6(\mu\text{-}OH)_3]$ had been crystallographically characterized,[14] as well as the phenoxide analogue, $[Et_4N]_3[W_2(CO)_6(\mu\text{-}OPh)_3]$.[15]

Ellis and Rochfort[16] have reported the synthesis of a number of complexes of the general formula $[R_4N]_n[M(CO)_3OR]_n$ (n = 3,4; M = Cr, Mo, W; R = Me, Et) from the reaction of $M(CO)_3$PMTA (PMTA = 1,1,4,7,7-pentamethyldiethylenetriamine) with the corresponding NaOR reagent, followed by cation exchange with $[R_4N]Cl$. In the case of M = W, R = Et, a crystal structure was obtained, revealing the complex to be a trimer, $[W_3(CO)_9(\mu\text{-}OEt)(\mu_3\text{-}OEt)_2]^{3-}$. More recently Lin and co-workers have reported the synthesis and characterization of $[Et_4N]_4[M(CO)_3(\mu_3\text{-}OH)]_4$ (M = Mo, W) from the reaction of $M(CO)_3$(PMTA) with a stoichiometric quantity of hydroxide ion in aqueous THF solutions.[17] These complexes were shown to be isostructural with the chromium analogue.[18]

Previously, McNeese and co-workers have prepared some polynuclear chromium alkoxide derivatives, $[Et_4N]_4[Cr_4(CO)_{12}(OR)_4]$ (R = H, Me).[18] These complexes were synthesized by the reaction of excess hydroxide ion with chromium hexacarbonyl in the presence of water and methanol, respectively (eq 4). The structure of the anion is a tetrameric arrangement of

$$Cr(CO)_6 + Et_4NOH \xrightarrow[R = H, Me]{ROH} [Et_4N]_4[Cr(CO)_3(OR)]_4 \quad (4)$$

chromium tricarbonyl units and alkoxide ligands forming alternate corners of a distorted cube (Figure 1). In addition the phenoxide tetramer, $[Cr_4(CO)_{12}(OPh)_4]^{4-}$, was prepared by the reaction of $Cr(CO)_3(CH_3CN)_3$ with an equimolar amount of $[Et_4N][OPh]$ or by refluxing $[Et_4N][OPh]$ with $Cr(CO)_6$ in THF. These tetrameric derivatives were believed to be formed from CO loss in $Cr(CO)_5OR^-$ intermediates followed by aggregation. However, attempts to spectroscopically observe these monomers during the syntheses were unsuccessful.

It is apparent from the above discussion that there are two major problems that must be overcome to isolate monomeric $M(CO)_5OR^-$ derivatives. These are the reversible nature of reaction 1, where the mononuclear group 6 metal alkoxides are unstable with respect to formation of the metal hydride and corresponding aldehyde or ketone, and the propensity of these monomeric species to aggregate to dimers or higher nuclearity clusters. In this report we wish to describe the syntheses and structures of zerovalent group 6 metal aryl oxide and their reactivity toward carbon dioxide.[19] We have avoided the difficulty of the reversible nature of reaction 1 by employing aryl oxides as ligands and have overcome the second obstacle by carrying out the chemistry under an atmosphere of carbon monoxide.

Experimental Section

Materials and Methods. All reactions were carried out under a dry nitrogen atmosphere on a double-manifold Schlenk vacuum line. Solid transfers were performed under a stream of nitrogen or in an argon-filled drybox. Solvents were dried by distillation from the appropriate reagents and deoxygenated prior to use. Infrared spectra were recorded in 0.10-mm CaF_2 cells on a IBM FT-IR Model 32 spectrometer. ^1H and ^{13}C NMR spectra were recorded on a Varian XL-200E spectrometer.

Synthesis of Compounds. [Na][OPh]. Approximately 1 g of sodium metal was added to a solution of phenol (in excess) in diethyl ether at 0 °C in an ice bath.[20] The solution was stirred overnight during which time it gradually warmed up to ambient temperature. A white solid formed which was isolated by reducing the solution's volume by half, filtering through a medium porosity frit, and washing the solid with 1:1 ether/hexane by volume. This preparation leaves any excess phenol in solution. The solid was used without further purification.

[PPN][OPh]. NaOPh (0.95 g, 8.2 mmol) and PPNCl (4.68 g, 8.2 mmol) (PPN = bis(triphenylphosphino)iminium, $Ph_3P{=}N{=}PPh_3$) were stirred in 30 mL of methanol for 6 h. After the methanol was removed under vacuum, the residue was extracted into 15 mL of acetone, leaving behind NaCl as a white solid. The acetone solution was filtered, and the crude product precipitated upon the addition of diethyl ether. The product was purified by two recrystallizations from acetone/ether to yield 3.95 g (76.6% yield) of product. ^1H NMR ($(CD_3)_2CO$): cation $(Ph_3P)_2N^+$ δ 7.52–7.85 m; anion $C_6H_5O^-$ 6.52–6.93 m. Relative intensities, cation:anion; predicted 6:1; observed 6.1:1.

[Et$_4$N][OPh]. This material was synthesized according to the procedure reported by McNeese and co-workers.[18] Phenol (6.67 g, 0.071 mol) was dissolved in 50 mL of dry methanol in a 200-mL round-bottom flask, and Et_4NOH in methanol (25% w/w; 43.8 g, 0.074 mol OH^-) was added to the solution. The flask was fitted with a reflux condenser, and the solution was heated to 65 °C for 2 h. After the solution was cooled, the methanol was pumped off under vacuum. The product was extracted from the resulting residue with THF/CH_3CN (6:1 v/v) and filtered. Cooling to −11 °C caused the precipitation of white crystals of $[Et_4N][OPh]$, 13.6 g, 86% yield. ^1H NMR (CD_3CN): cation CH_3 (t) δ 1.17, CH_2 (q) 3.16; anion C_6H_5 (t) 6.12, (d) 6.50, (t) 6.83. ^{13}C NMR (CD_3CN): cation CH_3 δ 7.73, CH_2 52.89; anion C_6H_5 110.1, 119.3, 129.7, 170.9.

[Et$_4$N][OC$_6$H$_4$CH$_3$-*m*]. The same method was followed as for the preparation of $[Et_4N][OPh]$. *m*-Cresol (7.52 g, 0.0695 mol) was heated in methanol with Et_4NOH (25% in MeOH, 43.92 g, 0.0746 mol of OH^-). The product was isolated as described above and recrystallized twice from CH_3CN and THF. Yield of product was 8.40 g, 50.9%. ^1H NMR (CD_3CN): cation CH_3 (t) δ 1.15, CH_2 (q) 3.17; anion $C_6H_4CH_3$ (s) 2.10, $C_6H_4CH_3$ (d) 5.95, (d) 6.10, (s) 6.16, (t) 6.73. ^{13}C NMR (CD_3CN): cation CH_3 δ 7.5, CH_2 52.6; anion $C_6H_4CH_3$ 21.8, $C_6H_4CH_3$ 111.2, 116.2, 119.8, 129.3, 138.5, 170.6.

[Et$_4$N][Cr(CO)$_5$OPh]. $Cr(CO)_6$ (0.452 g, 2.05 mmol) dissolved in 55 mL of THF was irradiated with a 450-W mercury vapor lamp under a nitrogen purge in a water-cooled photocell for 60 min to produce $Cr(CO)_5THF$ (IR (THF) 2074 (w), 1939 (s), 1895 (m) cm^{-1}). The $Cr(CO)_5THF$ solution was transferred by cannula to a flask containing 0.472 g (2.11 mmol) of $[Et_4N][OPh]$. Upon stirring the solution for 5–10 min

(9) (a) Darensbourg, D. J.; Pala, M.; Rheingold, A. L. *Inorg. Chem.* **1986**, *25*, 125. (b) Darensbourg, D. J.; Pala, M.; Simmons, D.; Rheingold, A. L. *Inorg. Chem.* **1986**, *25*, 3537.
(10) Hieber, W.; Rieger, K. *Z. Anorg. Allg. Chem.* **1959**, *300*, 288.
(11) Hieber, W.; Englert, K.; Rieger, K. *Z. Anorg. Allg. Chem.* **1959**, *300*, 295.
(12) Hieber, W.; Englert, K.; Rieger, K. *Z. Anorg. Allg. Chem.* **1959**, *300*, 304.
(13) Hieber, W.; Englert, K. *Z. Anorg. Allg. Chem.* **1959**, *300*, 311.
(14) Albano, V. G.; Ciana, G.; Manassero, M. *J. Organomet. Chem.* **1970**, *25*, C55.
(15) Darensbourg, D. J.; Sanchez, K. M.; Reibenspies, J. H. *Inorg. Chem.* **1988**, *27*, 3269.
(16) Ellis, J. E.; Rochfort, G. L. *Organometallics* **1982**, *1*, 682.
(17) Lin, J. T.; Yeh, S. K.; Lee, G. H.; Wang, Y. *J. Organomet. Chem.* **1989**, *361*, 89.
(18) (a) McNeese, T. J.; Cohen, M. B.; Foxman, B. M. *Organometallics* **1984**, *3*, 552. (b) McNeese, T. J.; Mueller, T. E.; Wierda, D. A.; Darensbourg, D. J.; Delord, T. J. *Inorg. Chem.* **1985**, *24*, 3465.
(19) Darensbourg, D. J.; Sanchez, K. M.; Rheingold, A. L. *J. Am. Chem. Soc.* **1987**, *109*, 290.
(20) Mascharak, P. K.; Armstrong, W. H.; Mizobe, Y.; Holm, R. H. *J. Am. Chem. Soc.* **1983**, *105*, 475.

at 0 °C, the desired product formed. The solution was maintained at 0 °C to avoid decomposition. IR of $[Et_4N][Cr(CO)_5OPh]$ (THF) 2056 (w), 1915 (s), 1856 (m) cm^{-1}. Reactions using this compound were performed from freshly prepared solutions, keeping the temperature at 0 °C by using an ice bath. Attempts at isolation of the pentacarbonyl complex were unsuccessful.

$[Et_4N][Cr(CO)_5COOPh]$. Tetrahydrofuran (25 mL) was added to a 100-mL Schlenk flask containing 0.221 g (1.01 mmol) of $Cr(CO)_6$ and 0.254 g (1.14 mmol) of $[Et_4N][OPh]$. The solution was stirred at ambient temperature while the formation of $Cr(CO)_5COOPh^-$ was monitored by infrared spectroscopy. As the intensity of the ν(CO) band for $Cr(CO)_6$ (1979 cm^{-1}) decreased, new bands grew in at 2020 (w), 1884 (s), 1860 (m, sh), and 1646 (mw, br, COOPh) cm^{-1}. After 3 h, a secondary product with IR bands at 2056 (w), 1915 (s), and 1856 (m) cm^{-1} became the major component of the solution. These bands are attributed to $Cr(CO)_5OPh^-$. Ultimately, the only compound isolable from this reaction is the tetranuclear species, $[Et_4N]_4[Cr_4(CO)_{12}(OPh)_4]$, which precipitates from the solution.

$[Et_4N]_4[Cr_4(CO)_{12}(OPh)_4]$. The complex $[Et_4N][Cr(CO)_5OPh]$ was prepared as described above, but instead of cooling the solution to 0 °C it was stirred at ambient temperature overnight. A considerable amount of precipitate formed in the solution during this time period. The solid was isolated by filtration and washed with acetone. Recrystallization was achieved by layering diethyl ether over a concentrated CH_3CN solution of the solid product. Amber-colored crystals of $[Et_4N]_4[Cr_4(CO)_{12}(OPh)_4]$ were collected that exhibited ν(CO) infrared bands at 1866 (s) and 1730 (vs) cm^{-1} in acetonitrile.

$[Et_4N][W(CO)_5OPh]$. $W(CO)_5THF$ was prepared by photolysis of $W(CO)_6$ (0.55 g, 1.6 mmol) in 55 mL of THF for 1 h (IR, ν(CO) in THF, 2076 (vw), 1931 (s), and 1892 (m) cm^{-1}). The $W(CO)_5THF$ solution was transferred via cannula to a flask containing Et_4NOPh (0.35 g, 1.6 mmol) and a stir bar. After approximately 10 min of stirring at room temperature, the $W(CO)_5THF$ had reacted to form the desired product, $[Et_4N][W(CO)_5OPh]$, in quantitative yield. The solution was cooled to 0 °C and placed under a carbon monoxide atmosphere to prevent decomposition. It was subsequently filtered through a medium-porosity frit under CO pressure to a second 100-mL Schlenk flask also maintained at 0 °C. $[Et_4N][W(CO)_5OPh]$ was precipitated as yellow-orange crystals at −11 °C upon slow layering of hexane to the THF solution. Anal. Calcd for $[Et_4N][W(CO)_5Ph]$: C, 41.70; H, 4.60; N, 2.56. Found: C, 41.93; H, 4.72; N, 2.47. IR (THF) 2057 (w), 1904 (s), and 1852 (m) cm^{-1}. ^1H NMR ($(CD_3)_2CO$): cation CH_3 (t) δ 1.30, CH_2 (q) 3.38; anion C_6H_5 (t) 6.56, (t) 6.86, (t) 7.04. ^{13}C NMR ($(CD_3)_2CO$/THF, carbonyls) 200.0 (4 C, J_{W-C} = 130 Hz), 203.6 (1 C). $[Et_4N][W(^{13}CO)_5OPh]$ was similarly prepared by allowing the solution of $[Et_4N][W(CO)_5OPh]$ to stand under an atmosphere of ^{13}CO for 5 h at 0 °C prior to precipitation.

$[PPN][W(CO)_5OPh]$. This complex was prepared in the same manner as the Et_4N^+ salt. [PPN][OPh] (0.392 g, 0.622 mmol) was reacted with the photochemically generated $W(CO)_5THF$ ($W(CO)_6$, 0.219 g, 0.623 mmol). The product was isolated and recrystallized as described previously for the $[Et_4N][W(CO)_5OPh]$ complex. Yellow blocklike crystals were obtained. IR (THF) 2061 (w), 1912 (s), 1846 (m) cm^{-1}. ^{13}C NMR ($THF/(CD_3)_2CO$, carbonyls (enriched in ^{13}CO by placing a atmosphere of ^{13}CO over a THF solution in an NMR tube and leaving the NMR tube overnight at −10 °C)) cis 200.0 (4 CO, J_{W-C} = 129.0 Hz), trans 204.6 (1 CO).

$[Et_4N][W(CO)_5COOPh]$. $W(CO)_6$ (0.239 g, 0.680 mmol) and $[Et_4N][OPh]$ (0.237 g, 1.06 mmol) were placed in a 100-mL Schlenk flask with a stir bar. THF (50 mL) was added as solvent. The formation of $W(CO)_5COOPh^-$ was monitored by infrared spectroscopy. After 20 min of reaction at room temperature, the major components of the solution were $W(CO)_6$ (IR ν(CO) = 1976 (s) cm^{-1}) and $W(CO)_5COOPh^-$ (IR bands ν(CO) = 2032 (w), 1889 (s), 1865 (ms, sh), COOPh = 1644 (w, br) cm^{-1}). The IR bands for $W(CO)_6$ and $W(CO)_5COOPh^-$ decreased in intensity over a period of several hours of reaction. A second set of bands grew in at 2057 (w), 1904 (s), and 1852 (m) cm^{-1}, which were identified as those of $W(CO)_5OPh^-$. These bands also decreased in intensity after several more hours. The major product isolated from this reaction was the tetrameric species, $[Et_4N]_4[W_4(CO)_{12}(OPh)_4]$, which precipitated from the solution.

$[Et_4N]_4[W_4(CO)_{12}(OPh)_4]$. This complex was prepared in a procedure similar to that of the chromium phenoxide tetramer. A solution of $[Et_4N][W(CO)_5OPh]$ (0.564 g, 1.03 mmol) in 40 mL of THF was stirred at room temperature for 2 days. The solution was filtered, and the solid was washed three times with 10 mL of acetone. The solid product was recrystallized twice at −10 °C from CH_3CN/Et_2O. IR (CH_3CN) ν(CO) 1853 (ms), 1718 (vs) cm^{-1}.

$[Et_4N][cis\text{-}Cr(CO)_4(PR_3)OPh]$ (PR_3 = PMe_3, $P(OMe)_3$). A freshly prepared solution of $[Et_4N][Cr(CO)_5OPh]$, 1.30 mmol in 40 mL of THF, was cooled to 0 °C to prevent decomposition to the tetramer. PR_3 (0.1 mL of PMe_3, 1.3 mmol, or 0.2 mL of $P(OMe)_3$, 1.7 mmol) is added to the solution via syringe. An infrared spectrum of the solution was immediately recorded, which revealed complete substitution of a carbonyl ligand by the phosphine to form the product, $[Et_4N][cis\text{-}Cr(CO)_4(PR_3)OPh]$. IR(THF) PR_3 = PMe_3 2001 (w), 1872 (s), 1809 (ms), PR_3 = $P(OMe)_3$ 1999 (w), 1883 (s), 1823 (ms) cm^{-1}. The products were precipitated upon the addition of ether and hexane to the solutions. The solids were washed with ether and then recrystallized from THF/ether/hexane.

$[Et_4N][cis\text{-}W(CO)_4(PR_3)OPh]$ (PR_3 = PMe_3, $P(OMe)_3$). A freshly prepared solution of $[Et_4N][W(CO)_5OPh]$ (from $W(CO)_5THF$ and Et_4NOPh or dissolving crystals of $[Et_4N][W(CO)_5OPh)]$ in THF was cooled to 0 °C. One equivalent of the phosphine was added to the solution via syringe. Monitoring the reaction by infrared spectroscopy revealed the complete formation of the products, $cis\text{-}W(CO)_4(PR_3)OPh^-$ within 10 min of stirring at 0 °C. The solutions were then filtered, and the products were precipitated upon addition of ether and hexane. The solids were washed with ether and recrystallized from acetone, ether, and hexane. IR (THF) PR_3 = PMe_3 1991 (w), 1863 (s), 1806 (m), PR_3 = $P(OMe)_3$ 2000 (w), 1868 (s), 1817 (m) cm^{-1}. ^{13}C NMR (CD_3CN/THF): cation CH_3 δ 6.48, CH_2 51.5; anion (carbonyls) 203.7 (2 CO, cis to phosphine and OPh ligands, J_{C-P} = 11.1 Hz), 207.2 (1 CO, cis to phosphine, trans to OPh, J_{C-P} = 5.4 Hz), 211.1 (1 CO, trans to phosphine, cis to OPh, J_{C-P} = 62.6 Hz).

$[Et_4N][cis\text{-}W(CO)_4(PPh_3)OPh]$. A solution of $[Et_4N][W(CO)_5OPh]$, prepared from 0.55 g (1.0 mmol) of complex in 45 mL of THF, was cooled to 0 °C in an ice bath, and solid PPh_3 (0.53 g, 2.0 mmol) was added to the solution under a stream of nitrogen. The reaction was monitored by infrared spectroscopy. After 1.8 h at 0 °C the reaction went to completion. The solution was filtered and the product was precipitated upon the addition of ether and hexane. Recrystallization from acetone/ether yielded bright yellow crystals of product which exhibited an IR spectrum in the ν(CO) region in THF with peaks at 1993 (m), 1867 (vs), and 1811 (m) cm^{-1}.

$[Et_4N][Cr(CO)_5O_2COPh]$. A freshly prepared tetrahydrofuran solution of $[Et_4N][Cr(CO)_5OPh]$ was degassed at 0 °C, and 1 atm of carbon dioxide was added. An infrared spectrum recorded immediately after the addition of CO_2 revealed the presence of the insertion product, $Cr(CO)_5O_2COPh^-$. The product was isolated by filtering after precipitation upon addition of hexane in the presence of a carbon dioxide atmosphere. IR (THF) ν(CO) 2060 (w), 1923 (s), 1859 (m) cm^{-1}. ^{13}C NMR ($THF/(CD_3)_2CO$) Cr−O−C(O)OPh δ 162.1 (using $^{13}CO_2$ in the synthesis).

$[Et_4N][Cr(CO)_5SC(O)OPh]$. This complex was prepared in the same manner as the chromium phenyl carbonate complex. A solution of $[Et_4N][Cr(CO)_5OPh]$ was reacted with 1 atm of carbonyl sulfide in a 100-mL Schlenk flask, at 0 °C in THF. A solid product was obtained upon addition of hexane to the THF solution. This product was recrystallized from acetone/ether/hexane. IR (THF) 2045 (w), 1919 (s), 1871 (m) cm^{-1}.

$[Et_4N][Cr(CO)_5S_2COPh]$. A freshly prepared solution of $[Et_4N][Cr(CO)_5OPh]$ (1.5 mmol in 45 mL of THF) was cooled to 0 °C, and carbon disulfide (0.5 mL, 8.3 mmol) was added to the solution. An infrared spectrum was immediately recorded, revealing the presence of the insertion product, $Cr(CO)_5S_2COPh^-$. The solution was filtered, and the product precipitated upon the addition of hexane. The resultant oil was washed with ether and recrystallized from acetone and ether to yield a maroon solid. IR (THF) 2052 (w), 1925 (s), 1880 (m) cm^{-1}.

$[Et_4N][W(CO)_5O_2COR]$ (R = Ph, $C_6H_4CH_3$-*m*). A solution of $[Et_4N][W(CO)_5OR]$ was prepared in a 100-mL Schlenk flask in THF. The solution was cooled to 0 °C in an ice bath, and the flask was evacuated and refilled with 1 atm of carbon dioxide. The insertion process was monitored by infrared spectroscopy. The IR bands were observed to gradually shift from the original positions of the starting material to the positions of the inserted product within 30 min of mixing. The solution was filtered, and CO_2 was again added to the flask. The product was precipitated upon the addition of hexane at −10 °C to yield a pale yellow solid. $[Et_4N][W(CO)_5O_2COPh]$: IR (THF) 2063 (w), 1913 (s), 1854 (m) cm^{-1}. ^1H NMR (CD_3CN): δ cation CH_3 (t) 1.19, CH_2 (q) 3.22; anion C_6H_5 (m) 6.51–7.23. ^{13}C NMR (CD_3CN): δ cation CH_3 7.55, CH_2 52.91; anion C_6H_5 108.8, 116.6, 129.9, 155.9; O_2COPh 159.8 (identified by using $^{13}CO_2$ in the synthesis); carbonyls (THF/CD_3CN) 205.5 (4 CO, J_{W-C} = 124.5 Hz), 209.4 (1 CO) (using $W(^{13}CO)_5OPh^-$ in the synthesis). $[Et_4N][W(CO)_5O_2COC_6H_4CH_3\text{-}m]$: IR (THF) 2062 (w), 1914 (s), 1855 (m). ^1H NMR ($(CD_3)CO$): δ cation CH_3 (t) 1.17, CH_2 (q) 3.16; anion $C_6H_4CH_3$ (s) 2.12, $C_6H_4CH_3$ (m) 5.87–6.78. ^{13}C NMR (CH_3CN/CD_3CN): δ cation CH_3 7.72, CH_2 52.85; anion $C_6H_4CH_3$ 21.90, $C_6H_4CH_3$ 110.7, 116.5, 120.2, 129.3, 138.5, 155.7; $O_2COC_6H_4CH_3$ 161.5 (identified by using $^{13}CO_2$ in the synthesis).

Table I. Crystallographic Data

	I	II	III
mol formula	$C_{19}H_{25}NO_6W$	$C_{19}H_{26}NO_{6.50}W$	$C_{21}H_{42}N_2O_8W$
formula wt	547.3	556.3	633.9
space group	$P\bar{1}$	$P2_1/c$	$P\bar{1}$
a, Å	9.416 (3)	17.545 (5)	10.513 (5)
b, Å	12.665 (2)	25.322 (8)	15.881 (10)
c, Å	18.371 (3)	10.337 (3)	8.130 (6)
α, deg	92.38 (1)		101.69 (6)
β, deg	94.50 (2)	102.52 (3)	92.12 (5)
γ, deg	95.85 (2)		83.25 (5)
V, Å^3	2168.3	4483 (2)	1319.8
temp, C°	23 (1)	0	23 (1)
Z	4	8	2
D(calcd), g cm^{-3}	1.68	1.648	1.596
radiation	Mo Kα (λ = 0.71073 Å)	Mo Kα (λ = 0.71073 Å)	Mo Kα (λ = 0.71073 Å)
μ, cm^{-1}	54.68	52.95	46.6
R	7.06%	6.91	2.92
wR	7.71%	5.60	3.01

[Et$_4$N][W(CO)$_5$SC(O)OPh]. This complex was prepared in the same manner as the CO_2 insertion products, from the reaction of [Et$_4$N][W(CO)$_5$OPh] with 1 atm of pressure of carbonyl sulfide in THF at 0 °C. The complex was recrystallized from acetone/ether/hexane to yield a yellow-brown solid material. IR (THF) 2059 (w), 1916 (s), 1859 (m) cm^{-1}. ^{13}C NMR (THF/CD$_3$CN): δ *S*COPh 175.2.

[Et$_4$N][W(CO)$_5$S$_2$COPh]. This complex was prepared in the manner as the chromium phenyl dithiocarbonate complex. A solution of [Et$_4$N][W(CO)5OPh] in THF was prepared and cooled to 0 °C. Carbon disulfide (5 equivalents) was added to the solution via syringe. The IR spectrum showed immediate shifts in all of the carbonyl bands due to the formation of the insertion product. The solution was filtered and crude product precipitated upon the addition of hexane. The product was recrystallized three times from acetone/ether/hexane to yield brown crystals of [Et$_4$N][W(CO)$_5$S$_2$COPh]. IR (THF) 2056 (w), 1918 (s), 1863 (m) cm^{-1}. ^{13}C NMR (CH$_3$CN/CD$_3$CN): δ cation *C*H$_3$ 7.69, *C*H$_2$ 53.04; anion *C*$_6$H$_5$ 115.3, 119.0, 129.0, 153.3; S$_2$*C*OPh 198.1; carbonyls 204.1 (4 CO), 205.4 (1 CO).

[Et$_4$N]$_2$[W(CO)$_4$CO$_3$]. The complex [Et$_4$N][W(CO)$_5$O$_2$COPh] or [Et$_4$N][W(CO)$_5$O$_2$COC$_6$H$_4$CH$_3$-*m*] was prepared as previously described. An atmosphere of CO_2 was placed over a solution of the CO_2-inserted complexes in THF. A small quantity of wet, degassed solvent, THF or acetone (containing about 0.5 equiv of water) was added to the solution. The solution was stirred overnight at room temperature during which an orange precipitate was formed. The precipitate was isolated by filtration and washed with several 5-mL portions of THF. Recrystallization from CH$_3$CN/Et$_2$O lead to the isolation of a yellow-orange powdery solid. This solid was dissolved in acetone and precipitated upon the slow layering of diethyl ether at −10 °C. Orange crystals of [Et$_2$N]$_2$[W(CO)$_4$CO$_3$]·H$_2$O were isolated. IR (CH$_3$CN) 1977 (w), 1839 (vs), 1820 (sh), 1784 (m) cm^{-1}. ^{1}H NMR (CD$_3$CN): δ C*H*$_3$ (t) 1.17, C*H*$_2$ (q) 3.16. ^{13}C NMR (CH$_3$CN/CD$_3$CN): δ cation *C*H$_3$ 7.73, *C*H$_2$ 52.94; anion, carbonyls 219.5 (2 CO, cis to CO), 230.3 (2 CO, trans to CO$_3$); *C*O$_3$ 160.8.

[Et$_4$N]$_2$[W(CO)$_4$(CO$_2$S)] and [Et$_4$N]$_2$[W(CO)$_4$S$_2$CO]. These complexes were prepared by the procedure used to prepare the W(CO)$_4$(CO$_3$)$^{2-}$ complex. A sample of the COS or CS_2 insertion product was dissolved in THF. Wet, deoxygenated THF or acetone was added to the solution, and the solution was stirred overnight. The hydrolyzed products were formed, generally as brown oils. The solution above the oil was removed via cannula. The oil was washed several times with THF, and the products were recrystallized from CH$_3$CN/Et$_2$O. A second recrystallization from acetone/ether yielded brown-yellow powders. [Et$_4$N]$_2$[W(CO)$_4$(CO$_2$S)]: IR (CH$_3$CN) 2000 (w), 1857 (vs), 1825 (sh), 1783 (m) cm^{-1}. [Et$_4$N]$_2$[W(CO)$_4$(S$_2$CO)]: IR (CH$_3$CN) 1990 (w), 1863 (vs), 1845 (sh), 1801 (m) cm^{-1}. ^{13}C NMR (CH$_3$CN/CD$_3$CN): δ cation *C*H$_3$ 7.40, *C*H$_2$ 52.83; anion, carbonyls 207.7 (2 CO, cis to S$_2$CO), 215.6 (2 CO, trans to S$_2$CO); S$_2$*C*O 200.0.

X-ray Structure Determination. The X-ray crystallographic experiments were performed on either a Nicolet R3m/V or Enraf-Nonius CAD4 diffractometer utilizing graphite-monochromated molybdenum Kα radiation (γ = 0.71073 Å) at or near ambient temperature. All crystallographic computations were carried out with the SHELXTL-PLUS program library supplied by Nicolet XRD. Crystal data and experimental conditions are provided in Table I.

I. [Et$_4$N][W(CO)$_5$OPh]. An orange-yellow prismatic crystal (0.30 × 0.10 × 0.15 mm) was mounted in a glass capillary. To check crystal quality, ω scans of several intense reflections were measured. The width at half-height was 0.30° with a takeoff angle of 2.8°, indicating a good crystal quality. Cell constants and an orientation matrix for data collection, obtained from a least-squares refinement using the setting angles of 25 carefully centered reflections in the range $6 < 2\theta < 20°$, corresponding to the crystal being in the triclinic system with space group $P1$ or $P\bar{1}$. Cell dimensions were determined to be a = 9.416 (3) Å, b = 12.665 (2) Å, c = 18.371 (3) Å, α = 92.38 (1)°, β = 94.50 (2)°, γ = 95.85 (2)°, V = 2174.2 Å^3.

All data collection was performed at the Molecular Structure Corp., College Station, TX. Preliminary examination and data collection were performed with Mo Kα radiation (λ = 0.71073 Å) on an Enraf-Nonius CAD4 computer controlled κ axis diffractometer equipped with a graphite crystal, incident beam monochromator. The data were collected at 23 ± 1 °C by using the ω–2θ scan technique. A fixed scan rate of 6.7°/min (in ω) was used. Data were collected to a maximum of 2θ of 50°. The scan range (in degrees) was determined as a function of θ to correct for the separation of the Kα doublet. The scan width was calculated as follows:

$$\text{scan width} = 0.7 \pm 0.350 \tan \theta$$

Moving-crystal moving-counter background counts were made by scanning an additional 25% above and below this range. The ratio of peak counting time to background counting time was 2:1. The counter aperture was also adjusted as a function of θ. The horizontal aperture width ranged from 2.0 to 2.5 mm. The vertical aperture was set at 2.0 mm. The diameter of the incident beam collimator was 0.7 mm and the crystal to detector distance was 21 cm. For intense reflections, an attenuator was automatically inserted in front of the detector. The attenuator factor was 20.7.

A total of 7751 reflections were collected. The intensities of three representative reflections which were measured after every 150 reflections remained constant throughout data collection, indicating crystal and electronic stability. A series of ψ scans was collected.

The structure was solved by direct methods and subsequent difference Fourier syntheses. The tungsten atoms were refined with anisotropic thermal parameters. Hydrogen atoms were treated as idealized isotropic contributions, and their isotropic values were fixed at 0.05; C–H distances = 0.96 Å. The phenyl rings of the anions were constrained to rigid, planar hexagons.

II. [Et$_4$N][W(CO)$_5$OPh·0.5H$_2$O]. An orange-yellow prismatic crystal (0.25 × 0.15 × 0.20 mm) was mounted in a glass capillary. The intensity measurements were carried out with a Nicolet R3V diffractometer with graphite-monochromated Mo Kα radiation (λ = 0.71073 Å) at 0 °C. A total of 2794 reflections, with $I/T(I) = 3.0$, having $4.0 \le 2\theta \le 40°$ were measured. The 1.0°-wide ω-scan technique was used with a variable scan speed of 2.00–30.00°/min in 2θ and a background-to-scan ratio equal to 1.0. During the data collection, three standard reflections were monitored every 97 reflections.

Lorentz and polarization corrections were applied to the data. The unit cell parameters and the systematic absences are consistent with the monoclinic system, space group $P2_1/c$.

The structured was solved by direct methods in the $P2_1/c$ space group and subsequent difference Fourier syntheses. All non-hydrogen atoms were refined with anisotropic thermal parameters. Anomalous dispersion corrections and scattering factors were taken from the literature.[21] The positions of the hydrogen atoms were calculated by using an idealized sp^3-hydridized geometry and a C–H bond length of 0.960 Å. Refinement with a data: parameter ratio equal to 8.6 gave R_1 and R_2 values of 6.91% and 5.60% with a goodness of fit of 1.33.

III. [Et$_4$N]$_2$[W(CO)$_4$CO$_3$]·H$_2$O. An orange platelike crystal (0.30 × 0.20 × 0.10 mm) was mounted in a glass capillary in a random orientation. As a check on crystal quality, ω scans of several intense reflections were measured; the width at half-height was 0.25° with a takeoff angle of 2.8°, indicating good crystal quality. Preliminary examination and data collection were performed with Mo Kα radiation (λ = 0.71073 Å) on an Enraf-Nonius CAD4 computer κ axis diffractometer equipped with a graphite crystal, incident beam monochromator at the Molecular Structures Corp., College Station, TX. The data were collected at 23 ± 1 °C by using the ω–θ scan technique. A fixed scan rate of 6.7°/min (in ω) was used. Data were collected to a maximum 2θ of 50°. The scan range (in degrees) was determined as a function of θ to correct for the separation of the Kα doublet, and the scan width was calculated as follows: scan width = 0.7 ± 0.350 tan θ. Moving-crystal moving-counter background counts were made by scanning an additional 25% above and below this range. Thus, the ratio of peak counting time to background counting time was 2:1. The counter aperture was also adjusted as a

(21) *International Tables for X-Ray Crystallography*; Kynoch: Birmingham, England, 1974; Vol. IV.

Scheme II

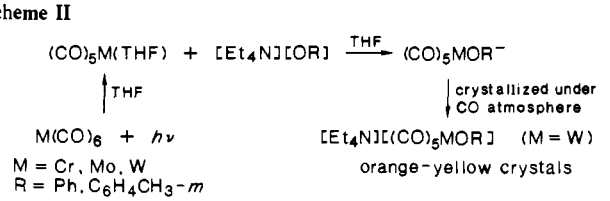

function of θ. The horizontal aperture width ranged from 2.0 to 2.5 mm, the vertical aperture set at 2.0 mm. The diameter of the incident beam collimator was 0.7 mm, and the crystal-to-detector distance was 21 cm. For intense reflections an attenuator was automatically inserted in front of the detector; the attenuator factor was 20.7.

A total of 4812 reflections were collected. As a check on crystal and electronic stability, three representative reflections were measured every 41 min. Lorentz and polarization corrections were applied to the data. A series of ψ scans were collected.

The crystal system was determined to be triclinic with space group $P1$ or $P\bar{1}$. The centrosymmetric space group alternative, $P\bar{1}$, was initially assumed and later proved correct by the chemically reasonable and well-behaved solution and refinement of the structure. The intensity data were empirically corrected for absorption. The structure was solved by heavy-atom methods and worked up by subsequent difference Fourier syntheses. A molecule of water cocrystallizes with the salt. All hydrogen atoms were located and isotropically refined. All non-hydrogen atoms were refined with anisotropic temperature factors. All computer programs are contained in the SHELXTL program library.

Results and Discussion

Synthesis of $M(CO)_5OR^-$ Derivatives. The synthetic method for generating the mononuclear aryl oxide complexes are summarized in Scheme II. Photolysis of the metal hexacarbonyl in THF produces the THF adduct of the metal pentacarbonyl, with subsequent replacement of the very labile THF ligand by OR^- to produce the $M(CO)_5OR^-$ complexes. Infrared data in the CO stretching region of these derivatives are provided in the Experimental Section and Table 2S in the supplementary material (see the paragraph at the end of the paper).

The $M(CO)_5OR^-$ complexes are unstable and decompose via loss of CO ligands to form binuclear $[M_2(CO)_6(OR)_3]^{3-}$ (M = W, excess OR^- present)[15] or tetranuclear $[M_4(CO)_{12}(OR)_4]^{4-}$ (M = Cr, Mo, W) species.[18] The stability of the $M(CO)_5OR^-$ complexes follows the trend W > Cr > Mo. Significant amounts of $Mo(CO)_5OR^-$ derivatives are never present in solution, even if temperatures are maintained at or below 0 °C. The lack of stability of $Mo(CO)_5OR^-$ has prevented further study into the reactivity of these complexes. On the other hand the chromium complexes, $Cr(CO)_5OR^-$ (R = Ph, $C_6H_4CH_3$-*m*), once formed are stable in solutions maintained below 0 °C for 30–45 min.

The tungsten pentacarbonyl aryl oxides are by far the most robust of the $M(CO)_5OR^-$ complexes. The solution half-life of the tungsten phenoxide complex, $W(CO)_5OPh^-$, is approximately 3 h at ambient temperature. Nevertheless, solutions of these complexes were also maintained at temperatures ≤0 °C for most reactivity studies. Isolation of the tungsten aryloxide complexes was accomplished by precipitation from carbon monoxide saturated solutions. The $W(CO)_5OR^-$ solutions were filtered under a CO atmosphere, and the solutions were cooled to 0 °C and resaturated with CO. Slow layering of hexane over THF solutions of $W(CO)_5OR^-$ at −10 °C led to the precipitation of yellow–orange needles of $[Et_4N][W(CO)_5OR]$ (R = Ph, $C_6H_4CH_3$-*m*). The phenyl derivative has been the subject of an X-ray crystallographic determination.

Although it was possible to isolate pure, crystalline samples of the $[Et_4N][W(CO)_5OR]$ derivatives by precipitation from solutions under a carbon monoxide atmosphere, it was not possible to similarly provide solid samples of the chromium and molybdenum analogues. This is due to the fact that the chromium and molybdenum mononuclear aryl oxide complexes are unstable in the presence of added carbon monoxide for extended time periods, decomposing to the parent hexacarbonyls.

On the other hand the $W(CO)_5OPh^-$ anion was unreactive toward CO in THF solution at ambient temperature and carbon monoxide pressures up to 500 psi (observed in situ in high-pressure CIR cell, Spectra Tech Inc.), with respect to either phenoxide displacement to afford $W(CO)_6$ or CO insertion to provide $W(CO)_5C(O)OPh^-$. This latter species was independently synthesized by nucleophilic addition of OPh^- to $W(CO)_6$ in tetrahydrofuran. However, phenoxide replacement by CO occurred upon heating $W(CO)_5OPh^-$ in THF in the CIR cell to 125 °C in the presence of carbon monoxide with concomitant production of $W(CO)_6$.

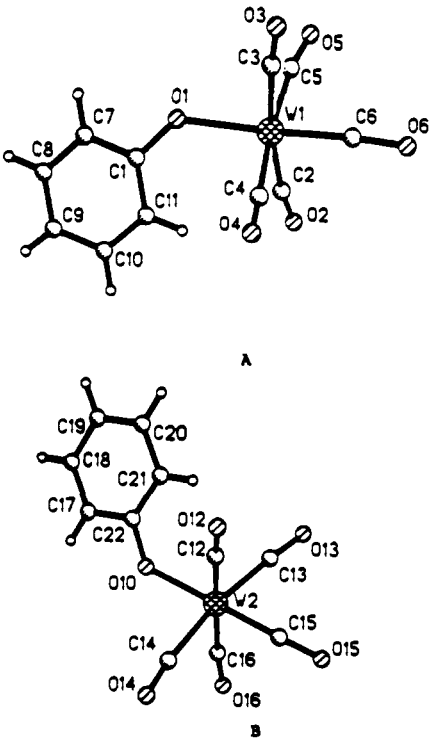

Figure 2. Molecular structure and labeling scheme for the $W(CO)_5OPh^-$ anions in complex I.

Table II. Bond Lengths (angstroms) of $[Et_4N][W(CO)_5OPh]$

W(1)–O(1)	2.181 (19)	W(1)–C(2)	2.023 (34)
W(1)–C(3)	2.045 (36)	W(1)–C(4)	2.011 (34)
W(1)–C(5)	1.983 (43)	W(1)–C(6)	1.841 (33)
O(1)–C(1)	1.335 (25)	C(2)–O(2)	1.131 (43)
C(3)–O(3)	1.117 (45)	C(4)–O(4)	1.166 (43)
C(5)–O(5)	1.169 (52)	C(6)–O(6)	1.247 (40)
W(2)–O(10)	2.203 (20)	W(2)–C(12)	2.054 (35)
W(2)–C(13)	1.930 (37)	W(2)–C(14)	2.009 (38)
W(2)–C(15)	1.908 (37)	W(2)–C(16)	2.017 (42)
O(10)–C(22)	1.316 (24)	C(12)–O(12)	1.156 (46)
C(13)–O(13)	1.188 (50)	C(14)–O(14)	1.194 (49)
C(15)–O(15)	1.210 (45)	C(16)–O(16)	1.163 (52)
N(1)–C(23)	1.511 (39)	N(1)–C(25)	1.472 (42)
N(1)–C(27)	1.523 (39)	N(1)–C(29)	1.519 (38)
C(23)–C(24)	1.499 (42)	C(25)–C(26)	1.516 (43)
C(27)–C(28)	1.491 (47)	C(29)–C(30)	1.500 (48)
N(2)–C(31)	1.474 (50)	N(2)–C(33)	1.474 (49)
N(2)–C(35)	1.490 (44)	N(2)–C(37)	1.499 (49)
C(31)–C(32)	1.497 (56)	C(33)–C(34)	1.612 (49)
C(35)–C(36)	1.526 (51)	C(37)–C(38)	1.517 (54)

Solid-State Structures of $[Et_4N][W(CO)_5OPh]$ (I) and $[Et_4N][W(CO)_5OPh\cdot 0.5H_2O]$ (II). Crystals of complex I were grown from a concentrated THF solution saturated with carbon monoxide upon the slow layering of hexane. The complex crystallized in the space group $P\bar{1}$ with two crystallographically independent cations and anions in the unit cell. Figure 2 illustrates the two independent $W(CO)_5OPh^-$ anions (A and B) with their respective atomic-labeling schemes. Bond distances and bond angles are contained in Tables II and III, respectively.

As is evident in Figure 2 the two anions possess the same gross structural features, with only slight differences in bond distances and angles being noted in the two species. The geometry about the tungsten atom is a slightly distorted octahedron with the

Table III. Bond Angles (degrees) of $[Et_4N][W(CO)_5OPh]$

O(1)-W(1)-C(2)	95.9 (11)	O(1)-W(1)-C(3)	91.2 (11)
C(2)-W(1)-C(3)	172.8 (13)	O(1)-W(1)-C(4)	95.5 (11)
C(2)-W(1)-C(4)	91.5 (13)	C(3)-W(1)-C(4)	89.0 (13)
O(1)-W(1)-C(5)	90.3 (13)	C(2)-W(1)-C(5)	90.5 (15)
C(3)-W(1)-C(5)	88.3 (15)	C(4)-W(1)-C(5)	173.6 (16)
O(1)-W(1)-C(6)	176.3 (11)	C(2)-W(1)-C(6)	85.9 (14)
C(3)-W(1)-C(6)	87.0 (14)	C(4)-W(1)-C(6)	87.6 (13)
C(5)-W(1)-C(6)	86.5 (15)	W(1)-O(1)-C(1)	130.8 (14)
W(1)-C(2)-O(2)	172.0 (29)	W(1)-C(3)-O(3)	174.7 (29)
W(1)-C(4)-O(4)	177.2 (24)	W(1)-C(5)-O(5)	169.6 (36)
W(1)-C(6)-O(6)	175.0 (26)	O(1)-C(1)-C(7)	117.4 (11)
O(1)-C(1)-C(11)	122.5 (11)	O(10)-W(2)-C(12)	95.7 (10)
O(10)-W(2)-C(13)	96.0 (11)	C(12)-W(2)-C(13)	89.9 (14)
O(10)-W(2)-C(14)	92.5 (12)	C(12)-W(2)-C(14)	92.1 (14)
C(13)-W(2)-C(14)	171.0 (14)	O(10)-W(2)-C(15)	178.4 (12)
C(12)-W(2)-C(15)	85.8 (14)	C(13)-W(2)-C(15)	83.4 (14)
C(14)-W(2)-C(15)	88.0 (15)	O(10)-W(2)-C(16)	88.3 (12)
C(12)-W(2)-C(16)	174.6 (12)	C(13)-W(2)-C(16)	93.2 (15)
C(14)-W(2)-C(16)	84.0 (15)	C(15)-W(2)-C(16)	90.2 (16)
W(2)-O(10)-C(22)	134.2 (15)	W(2)-C(12)-O(12)	177.5 (26)
W(2)-C(13)-O(13)	176.0 (33)	W(2)-C(14)-O(14)	167.1 (31)
W(2)-C(15)-O(15)	172.2 (31)	W(2)-C(16)-O(16)	168.6 (33)
O(10)-C(22)-C(17)	117.6 (12)	O(10)-C(22)-C(21)	122.3 (12)
C(23)-N(1)-C(25)	112.6 (23)	C(23)-N(1)-C(27)	112.4 (21)
C(25)-N(1)-C(27)	106.3 (24)	C(23)-N(1)-C(29)	106.2 (23)
C(25)-N(1)-C(29)	109.4 (22)	C(27)-N(1)-C(29)	109.9 (22)
N(1)-C(23)-C(24)	113.6 (26)	N(1)-C(25)-C(26)	115.5 (26)
N(1)-C(27)-C(28)	114.7 (26)	N(1)-C(29)-C(30)	115.2 (27)
C(31)-N(2)-C(33)	113.8 (29)	C(31)-N(2)-C(35)	109.0 (26)
C(33)-N(2)-C(35)	102.2 (27)	C(31)-N(2)-C(37)	110.7 (29)
C(33)-N(2)-C(37)	112.0 (27)	C(35)-N(2)-C(37)	108.6 (27)
N(2)-C(31)-C(32)	115.0 (33)	N(2)-C(33)-C(34)	112.3 (30)
N(2)-C(35)-C(36)	114.9 (31)	N(2)-C(37)-C(38)	115.6 (31)

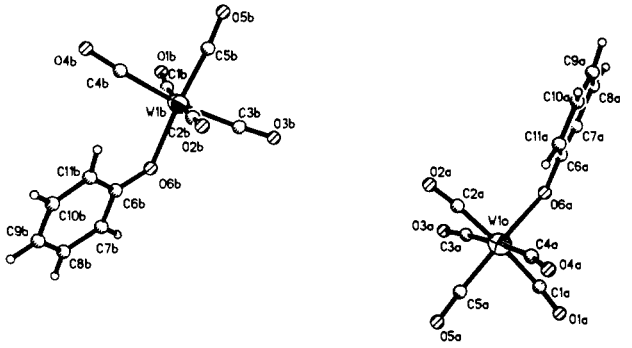

Figure 3. Molecular structure and labeling scheme for the $W(CO)_5OPh^-$ anions in complex II.

distortion presumably arising from steric interaction of the phenoxide ligand. This is seen in the OC_{cis}-W-O bond angles, which span the range 88.3–96.0°, where the largest deviations from 90° involve the carbonyl ligands closest in proximity to the phenoxide ligand, i.e., in anion A O(1)-W(1)-C(2) and O(1)-W(1)-C(4) and in anion B O(10)-W(2)-C(12) and O(10)-W(2)-C(13). The tungsten–carbon bonds trans to the phenoxide ligand are shorter than the tungsten–carbon bonds cis to the phenoxide group (e.g., in anion A, $W-C_{cis}$(av) = 2.016 [37] Å and $W-C_{trans}$ = 1.841 (33)). Hence, the phenoxide ligand exerts a trans influence comparable to that seen for the acetate and formate ligands in analogous W(0) complexes.

The tungsten–oxygen bond distances in the anions A and B are 2.181 (19) and 2.203 (20) Å, averaging 2.192 [20] Å. These distances are quite similar to the sum of the single-bond radii of the tungsten and oxygen atoms. Nevertheless, the W–O–C bond angle of 130.8 (14)° in A and 134.2 (15)° in B is indicative of significant π-donor interaction of the lone pair of the phenoxide ligand with the tungsten metal center. Indeed, this type of interaction might account for the enhanced substitutional lability of CO ligands in $W(CO)_5OPh^-$ (vide supra).

Crystals of complex II were similarly grown from a carbon monoxide saturated THF solution following the slow layering with hexane. Evidently there was a small quantity of water present in the particular batch of $[Et_4N][OPh]$ used in this synthesis. The complex crystallized in the space group $P2_1/c$ with two crystallographically independent cations and anions in the unit cell. Figure 3 illustrates the two independent $W(CO)_5OPh^-$ anions with their respective atomic-labeling schemes. The bond distances and bond angles are contained in Tables IV and V.

It is apparent upon a close examination of Tables IV and V that there are only small differences in intramolecular bond distances and angles among the two independent anions and cations in complex II. Similarly, there are no significant differences between the anions, $W(CO)_5OPh^-$, in structure II and

Table IV. Bond Lengths (angstroms) of $[Et_4N][W(CO)_5OPh\cdot0.5H_2O]$

W(1A)-C(1A)	2.006 (26)	W(1A)-C(2A)	1.927 (28)
W(1A)-C(3A)	2.016 (26)	W(1A)-C(4A)	1.961 (24)
W(1A)-C(5A)	1.904 (35)	W(1A)-O(6A)	2.224 (15)
C(1A)-O(1A)	1.155 (32)	C(2A)-O(2A)	1.208 (35)
C(3A)-O(3A)	1.142 (32)	C(4A)-O(4A)	1.186 (30)
C(5A)-O(5A)	1.153 (40)	O(6A)-C(6A)	1.339 (27)
C(6A)-C(7A)	1.368 (35)	C(6A)-C(11A)	1.387 (30)
C(7A)-C(8A)	1.411 (34)	C(8A)-C(9A)	1.343 (33)
C(9A)-C(10A)	1.349 (36)	C(10A)-C(11A)	1.402 (33)
W(1B)-C(1B)	1.978 (24)	W(1B)-C(2B)	1.991 (22)
W(1B)-C(3B)	1.991 (29)	W(1B)-C(4B)	2.001 (26)
W(1B)-C(5B)	1.891 (26)	W(1B)-O(6B)	2.190 (14)
C(1B)-O(1B)	1.187 (29)	C(2B)-O(2B)	1.167 (29)
C(3B)-O(3B)	1.160 (36)	C(4B)-O(4B)	1.176 (32)
C(5B)-O(5B)	1.191 (31)	O(6B)-C(6B)	1.323 (27)
C(6B)-C(7B)	1.396 (29)	C(6B)-C(11B)	1.394 (28)
C(7B)-C(8B)	1.403 (35)	C(8B)-C(9B)	1.369 (34)
C(9B)-C(10B)	1.340 (35)	C(10B)-C(11B)	1.332 (33)
N(1A)-C(12A)	1.494 (27)	N(1A)-C(14A)	1.560 (28)
N(1A)-C(16A)	1.536 (29)	N(1A)-C(18A)	1.503 (34)
C(12A)-C(13A)	1.507 (33)	C(14A)-C(15A)	1.500 (38)
C(16A)-C(17A)	1.512 (31)	C(18A)-C(19A)	1.461 (36)
N(1B)-C(12B)	1.526 (37)	N(1B)-C(14B)	1.494 (40)
N(1B)-C(16B)	1.511 (35)	N(1B)-C(18B)	1.481 (48)
C(12B)-C(13B)	1.461 (45)	C(14B)-C(15B)	1.507 (50)
C(16B)-C(17B)	1.519 (40)	C(18B)-C(19B)	1.541 (49)

Table V. Bond Angles (degrees) of $[Et_4N][W(CO)_5OPh\cdot0.5H_2O]$

C(1A)-W(1A)-C(2A)	174.6 (11)	C(1A)-W(1A)-C(3A)	91.3 (10)
C(2A)-W(1A)-C(3A)	90.4 (11)	C(1A)-W(1A)-C(4A)	89.7 (10)
C(2A)-W(1A)-C(4A)	88.3 (11)	C(3A)-W(1A)-C(4A)	176.0 (12)
C(1A)-W(1A)-C(5A)	89.3 (12)	C(2A)-W(1A)-C(5A)	85.6 (12)
C(oA)-W(1A)-C(5A)	88.7 (12)	C(4A)-W(1A)-C(5A)	87.4 (12)
C(1A)-W(1A)-O(6A)	86.2 (8)	C(2A)-W(1A)-O(6A)	99.0 (9)
C(3A)-W(1A)-O(6A)	86.3 (9)	C(4A)-W(1A)-O(6A)	97.6 (9)
C(5A)e-W(1A)-O(6A)	173.3 (9)	W(1A)-C(1A)-O(1A)	174.8 (23)
W(1A)-C(2A)-O(2A)	174.2 (23)	W(1A)-C(3A)-O(3A)	170.4 (26)
W(1A)-C(4A)-O(4A)	171.4 (23)	W(1A)-C(5A)-O(5A)	175.4 (27)
W(1A)-O(6A)-C(6A)	131.7 (14)	O(6Ae-C(6A)-C(7A)	117.2 (20)
O(6A)-C(6A)-C(11A)	121.7 (22)	C(7A)-C(6A)-C(11A)	121.0 (21)
C(6A-C(7A)-C(8A)	118.4 (22)	C(7A)-C(8A)-C(9A)	121.1 (24)
C(8A)-C(9A)-C(10A)	119.9 (23)	C(9A)-C(10A)-C(11A)	121.6 (22)
C(6A)-C(11A)-C(10A)	117.7 (22)	C(1B)-W(1B)-C(2B)	175.4 (10)
C(1B)-W(1B)-C(3B)	91.4 (11)	C(2B)-W(1B)-C(3B)	89.3 (10)
C(1B)-W(1B)-C(4B)	86.7 (10)	C(2B)-W(1B)-C(4B)	91.9 (10)
C(3B)-W(1B)-C(4B)	171.4 (10)	C(1B)-W(1B)-C(5B)	91.4 (10)
C(2B)-W(1B)-C(5B)	84.1 (10)	C(3B)-W(1B)-C(5B)	87.0 (11)
C(4B)-W(1B)-C(5B)	84.7 (11)	C(1B)-W(1B)-O(6B)	88.4 (8)
C(2B)-W(1B)-O(6B)	96.2 (7)	C(3B)-W(1B)-O(6B)	88.6 (8)
C(4B)-W(1B)-O(6B)	99.7 (8)	C(5B)-W(1B)-O(6B)	175.6 (9)
W(1B)-C(1B)-O(1B)	171.5 (19)	W(1B)-C(2B)-O(2B)	178.1 (20)
W(1B)-C(3B)-O(3B)	177.3 (21)	W(1B)-C(4B)-O(4B)	174.8 (17)
W(1B)-C(5B)-O(5B)	174.8 (22)	W(1B)-O(6B)-C(6B)	130.1 (11)
O(6B)-C(6B)-C(7B)	118.3 (17)	O(6Be-C(6B)-C(11B)	122.9 (17)
C(7B)-C(6B)-C(11B)	118.7 (20)	C(6B)-C(7B)-C(8B)	119.7 (19)
C(7B)-C(8B)-C(9B)	120.4 (22)	C(8B)-C(9B)-C(10B)	116.6 (26)
C(9B)-C(10B)-C(11B)	127.1 (23)	C(6B)-C(11B)-C(10B)	117.4 (19)
C(12A)-N(1A)-C(14A)	109.4 (16)	C(12A)-N(1A)-C(16A)	106.6 (16)
C(14A)-N(1A)-C(16A)	111.1 (17)	C(12A)-N(1A)-C(18A)	109.8 (18)
C(14A)-N(1A)-C(18A)	107.6 (16)	C(16A)-N(1A)-C(18A)	112.4 (17)
N(1A)-C(12A)-C(13A)	119.6 (20)	N(1A)-C(14A)-C(15A)	112.6 (18)
N(1A)-C(16A)-C(17A)	113.8 (19)	N(1A)-C(18A)-C(19A)	116.6 (19)
C(12B)-N(1B)-C(14B)	111.4 (23)	C(12B)-N(1B)-C(16B)	103.3 (20)
C(14B)-N(1B)-C(16B)	113.8 (24)	C(12B)-N(1B)-C(18B)	111.7 (26)
C(14B)-N(1B)-C(18B)	107.7 (23)	C(16B)-N(1B)-C(18B)	109.0 (25)
N(1B)-C(12B)-C(13B)	114.5 (25)	N(1B)-C(14B)-C(15B)	116.5 (24)
N(1B)-C(16B)-C(17B)	113.4 (22)	N(1B)-C(18B)-C(19B)	115.3 (26)

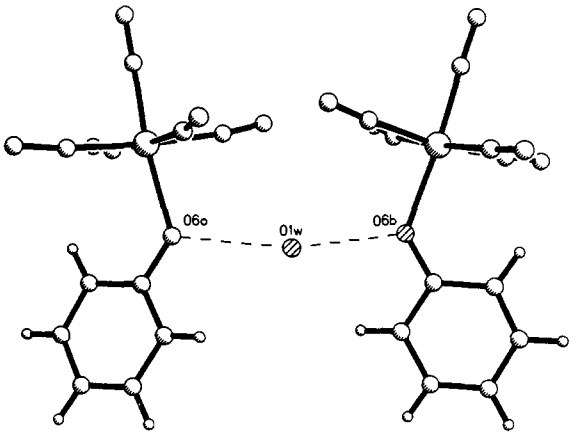

Figure 4. Hydrogen-bonding network in the $W(CO)_5OPh{\cdot}0.5H_2O$ anions in complex II.

in structure I, where there is not the presence of a water molecule. For example, the average W–OPh bond distance of 2.207 [15] Å and the average bond angle of 130.9 [13]° in species II are quite comparable to those reported for complex I. Figure 4 depicts the intermolecular hydrogen bonding between the water molecule and the ligated phenoxide ligands on two adjacent $W(CO)_5OPh^-$ anions. The O1w···O6b and O1w···O6a distances are 2.870 (20) and 2.878 (20) Å, respectively, with a O6a···O1w···O6b bond angle of 138.8 (10)°. Hence, the O–H···O linkage is nonlinear assuming the normal bond angles in H_2O. This intermolecular hydrogen bonding is observed in solution as well between alcohols and $W(CO)_5OPh^-$ (vide infra). The O···O distances, which average 2.874 [20] Å, are longer than those determined for intermolecular hydrogen bonds between metal-bound phenoxide and phenol in $(Me_3P)_3RhOR{\cdot}HOR$ (R = $C_6H_4CH_3$-*p*)[22] and $HPt(PCy_3)_2OPh{\cdot}HOPh$[23] of 2.62 and 2.64 Å, respectively.

Solution Reactivity of $M(CO)_5OR^-$ Anions. The CO-labilizing ability of the phenoxide ligand in the $(CO)_5W–OPh^-$ anion is amply demonstrated via reaction 5, where the anion is 100%

$$(CO)_5WOPh^- + {}^{13}CO \rightarrow ({}^{13}CO)_5WOPh^- + {}^{12}CO \quad (5)$$

enriched in ^{13}CO in 5 h at 0 °C in tetrahydrofuran. Reaction 5 is readily monitored by ^{13}C NMR spectroscopy with the cis carbonyl resonances occurring at 200.0 ppm (J_{W-C} = 130 Hz) and the trans carbonyl signal appearing at 204.6 ppm.

This CO displacement reaction occurs with equal facility when the incoming ligand is a phosphorus donor ligand. Addition of 1 equiv of trimethylphosphine or trimethyl phosphite to solutions of the chromium and tungsten pentacarbonyl phenoxide complexes leads to immediate and quantitative formation of the cis-metal tetracarbonylphosphine substituted phenoxide complexes. However, the reaction of $W(CO)_5OPh^-$ with PPh_3 proceeds much more slowly, with complete formation of the *cis*-$W(CO)_4(PPh_3)OPh^-$ complex occurring in about 2.5 h in the presence of 5-fold excess triphenylphosphine. This slow rate of formation of the PPh_3 derivative is due to a facile reverse reaction where the product complex readily reacts with CO to reform the parent $W(CO)_5OPh^-$ species.

The ^{13}C NMR spectrum of one of these substituted phenoxide derivatives, $[Et_4N][cis\text{-}W(CO)_4(P(OMe)_3)OPh]$, is depicted in Figure 5. The anion possesses three different types of carbonyl ligands. Each of these types of carbonyl groups has a set of ^{13}C NMR peaks which exhibit coupling to the phosphorus-31 nucleus and, in one instance, to the tungsten-183 nucleus. The assignment of the carbon resonances are based on intensity ratios and magnitude of the phosphorus coupling constants, in a manner consistent with assignments in related derivatives.[24]

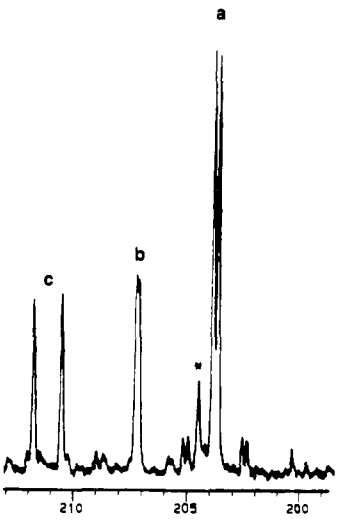

Figure 5. ^{13}C NMR spectrum for the *cis*-$W(CO)_4[P(OMe)_3]OPh^-$ anion in THF. Resonance a at 203.7 ppm (J_{C-P} = 11.1 Hz) is assigned to the two CO groups cis to both OPh and $P(OMe)_3$, peak b at 207.2 ppm (J_{C-P} = 5.4 Hz) is due to the CO group trans to OPh, and resonance c at 211.1 ppm (J_{C-P} = 62.6 Hz) is assigned to the CO group trans to $P(OMe)_3$. The signal marked with as asterisk is due to acetone.

Table VI. Infrared Data for Products of the Reaction of Et_4NOH/ROH with $M(CO)_6$ or $M(CO)_3(CH_3CN)_3$[a]

M	R	IR bands in CH_3CN, cm^{-1}	
		A_1 (s)	E (vs)
Cr	Ph[b]	1866 [1866]	1729 [1730]
Mo	Ph	1869 [1869]	1730 [1732]
W	Ph[c]	1861 [1853]	1725 [1718]
W	$C_6H_4CH_3$-m	1859 [1852]	1724 [1715]

[a] Data in brackets correspond to spectrum of product obtained from $M(CO)_5OR^-$, reaction 6. [b] Literature values for $[Et_4N]_4[Cr_4(CO)_{12}(OPh)_4]$ in CH_3CN: 1870 (s) and 1730 (vs) cm^{-1}.[18] [c] Literature values for $[Et_4N]_3[W_2(CO)_6(OPh)_3]$ in CH_3CN: 1860 (s) and 1719 (vs) cm^{-1},[16] and 1861 (s) and 1725 (vs) cm^{-1}.[15]

As previously mentioned, intermolecular hydrogen bonding of the ligated phenoxide ligand with alcohols is observed in CO-saturated solutions. That is, the ν(CO) infrared spectra of $W(CO)_5OPh^-$ in the presence of MeOH or PhOH exhibit shifts to higher frequency as a result of the decrease in donor strength of the phenoxide ligand (species A). For example, the ν(CO)

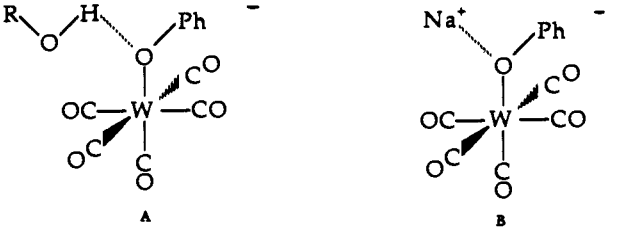

absorptions in THF (2057, 1904, and 1851 cm^{-1}) are displaced to 2059, 1913, and 1859 cm^{-1} upon addition of excess phenol; similarly the corresponding spectrum in methanol occurs at 2062, 1917, and 1863 cm^{-1}. Although, the interaction of MeOH with $W(CO)_5OPh^-$ does not result in formation of $W(CO)_5OMe^-$ and PhOH, the reverse reaction readily takes place, e.g., $[W_2(CO)_6(\mu_3\text{-}OMe)_3]^{3-}$ reacts with phenol to provide $[W_2(CO)_6(\mu_3\text{-}OPh)_3]^{3-}$.

An analogous interaction with sodium ion is noted in THF solution where the three-band ν(CO) pattern in $W(CO)_5OPh^-$ shifts to 2065, 1917, and 1862 cm^{-1} subsequent to the addition of 5 equiv of $NaBPh_4$. However, this ion-pairing interaction (species B) leads to displacement of the phenoxide ligand with

(22) Kegley, S. E.; Schaverein, C. J.; Freudenberger, J. H.; Bergman, R. J.; Nolan, S. P.; Hoff, C. D. *J. Am. Chem. Soc.* **1987**, *109*, 6563.
(23) Braga, D.; Sabatino, P.; DiBugno, C.; Leoni, P.; Pasquali, M. *J. Organomet. Chem.* **1987**, *334*, C46.
(24) Cotton, F. A.; Darensbourg, D. J.; Kolthammer, B. W. S.; Kudaroski, R. *Inorg. Chem.* **1982**, *21*, 1656.

concomitant formation of $W(CO)_6$ within 1 h at ambient temperature. In contrast, in the absence of sodium ion, solutions of the Et_4N^+ and PPN^+ salts of $W(CO)_5OPh^-$ are stable under a CO atmosphere for several months without significant accumulations of $W(CO)_6$.

In a deficiency of carbon monoxide, CO dissociation from the $M(CO)_5OR^-$ (R = Ph, $C_6H_4CH_3$-*m*) complexes results in aggregation to afford the tetrameric derivatives (eq 6). The tetramers were identified by their ν(CO) infrared spectra as compared with authentic samples synthesized by reaction 7 or 8 for M = Cr and Mo (Table VI). On the other hand reactions 7 and 8, for M = W, lead to the production of the dimer $[W_2(CO)_6(OR)_3]^{3-}$. Further reaction of the $[W_4(CO)_{12}(OR)_4]^{4-}$ species prepared via reaction 6 with OR^- yields the $[W_2(CO)_6(OR)_3]^{3-}$ dimer as well (eq 9).

$$4[Et_4N][M(CO)_5OR] \rightleftharpoons [Et_4N]_4[M_4(CO)_{12}(OR)_4] + 8CO \quad (6)$$

$$4M(CO)_3(CH_3CN)_3 + 4[Et_4N][OR] \xrightarrow[RT]{CH_3CN} [Et_4N]_4[M_4(CO)_{12}(OR)_4] \quad (7)$$

$$4M(CO)_6 + xs[Et_4N][OH] \xrightarrow[\Delta]{ROH} [Et_4N]_4[M_4(CO)_{12}(OR)_4] + 12CO \quad (8)$$

$$[W_4(CO)_{12}(OR)_4]^{4-} + 2OR^- \rightarrow 2[W_2(CO)_6(OR)_3]^{3-} \quad (9)$$

As indicated in eq 6, the reaction of monomers to provide tetramers and carbon monoxide is reversed in a CO atmosphere. The infrared spectra in the ν(CO) region clearly illustrate that the primary metal-containing species in solution upon reaction of the tetrameric or dimeric (in the case of M = W) anions with carbon monoxide in THF are the $M(CO)_5OR^-$ derivatives. Indeed, the reverse of eq 6, when R = Me or H, provides good routes to the corresponding $M(CO)_5OR^-$ derivatives.[25] These species are particularly unstable in the absence of a CO atmosphere. This chemistry will be the subject of a later publication.[26]

Insertion Reactions of $M(CO)_5OPh^-$ (M = Cr, W) with CO_2, COS, and CS_2. The reaction of carbon dioxide, carbonyl sulfide, and carbon disulfide with the metal pentacarbonyl phenoxide complexes produces the metal pentacarbonyl phenyl carbonate, phenyl thiocarbonate, and phenyl dithiocarbonate complexes, respectively. These reactions proceed readily under very mild conditions (0 °C; CO_2, COS pressure = 1 atm; CS_2 = 5–10 equiv). The reactions of the chromium complex with CO_2, COS, and CS_2 all occur within the time of mixing. The reactions of the tungsten complex with COS and CS_2 occur within 5 min of addition of the reagent, whereas reaction of $W(CO)_5OPh^-$ with CO_2 is complete within 30 min. In contrast, insertion of CO_2 into the tungsten carbon bond of $CH_3W(CO)_5^-$ requires several days under 1 atmosphere of carbon dioxide.[27]

The $M(CO)_5YC(X)OPh^-$ products have been spectroscopically characterized (see the Experimental Section). The COS insertion products are proposed to be metal bound through the sulfur atom, consistent with the insertion of COS into the $HCr(CO)_5^-$ complex to produce the sulfur-bound thioformate complex, $Cr(CO)_5SCHO$, as shown by X-ray crystallography.[28,29] The ^{13}C NMR spectra of the carbonate resonance shift downfield as one proceeds from the carbonate to the monothiocarbonate to the dithiocarbonate, analogous to previous observations on the corresponding formate derivatives.[29]

If the carbon dioxide insertion reaction of $W(CO)_5OPh^-$ is carried out in the presence of 2–10 atm of carbon monoxide, no $W(CO)_6$ is formed nor is the rate of carbon dioxide insertion altered. Hence, the phenoxide moiety remains in the coordination sphere of the metal during the insertion process and CO dissociation from the metal center is not rate determining. We propose that CO_2 behaves as an electrophile, interacting initially at the lone pair on the bound phenoxide in much the same manner as Na^+ ions or alcohols, with subsequent formation of the ligated phenyl carbonate (Scheme III).

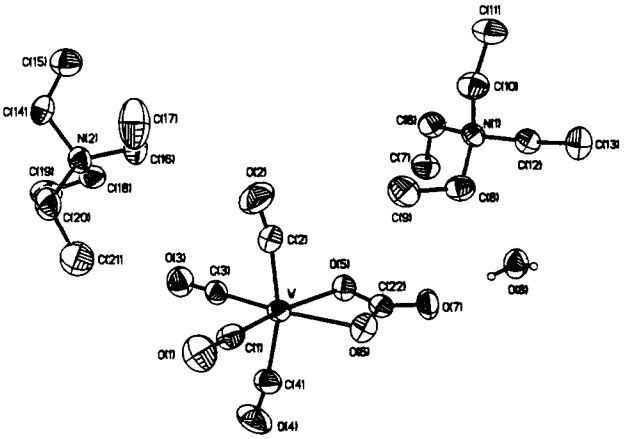

Figure 6. Molecular structure and labeling scheme for $[Et_4N]_2[W(CO)_4(CO_3)]\cdot H_2O$. The formula units are assembled as they occur in the unit cell.

Scheme III

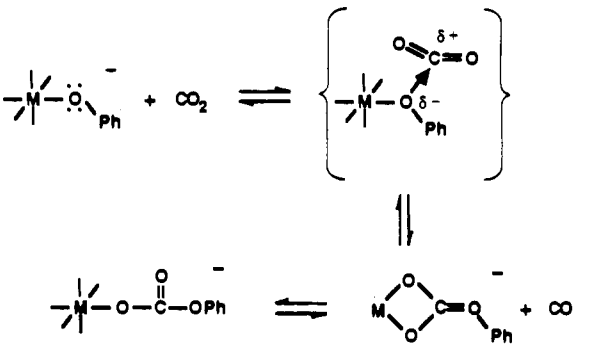

As indicated in Scheme III carbon dioxide insertion into the phenoxide–metal bond is reversible. For example, upon removal of the carbon dioxide atmosphere after a reaction has gone to completion, deinsertion occurs and the metal pentacarbonyl phenoxide complexes were observed to decompose to the corresponding $[M(CO)_3OR]_4^{4-}$ tetramers. Therefore, an atmosphere of CO_2 must be maintained over solutions of the aryl carbonates to isolate the products. No evidence for the reversible nature of COS and CS_2 insertion has been noted, at least at ambient temperatures. Such results reflect the stronger metal–sulfur bond, as compared with M–O bond, supporting the conclusion that COS insertion occurs with M–S bond formation.

The reversibility of the carbon dioxide insertion reaction (Scheme III) is consistent with our current view of the decarboxylation mechanism. That is, whether or not decarboxylation occurs appears to be strongly dependent on the nature of the X group in the [MOC(O)X] moiety. Decarboxylation is only observed where the X group has an appropriate orbital for interaction with the metal center during the decarboxylation process, e.g., when X = -H,[30] $-CH_2CN$,[31] -OR. A detailed analysis of the decarboxylation pathway is under way in our laboratories.

Qualitatively, there appears to be a significant retardation of the rate of carbon dioxide insertion as the metal center is made

(25) For example, the $M(CO)_5OMe^-$ derivatives (M = Cr, W) exhibit ν(CO) infrared bands at 1918 (s) and 1860 (m) cm^{-1} and 1908 (s) and 1851 (m) cm^{-1} in THF, respectively. The weak high-frequency band was not observed.

(26) Sanchez, K. M. Ph.D. Dissertation, 1988 Texas A&M University, College Station, TX.

(27) Darensbourg, D. J.; Hanckel, R. K.; Bauch, C. G.; Pala, M.; Simmons, D.; White, J. N. *J. Am. Chem. Soc.* **1985**, *107*, 7463.

(28) Darensbourg, D. J.; Rokicki, A. *J. Am. Chem. Soc.* **1982**, *109*, 349.

(29) Darensbourg, D. J.; Rokicki, A. *Organometallics* **1982**, *1*, 1685.

(30) Darensbourg, D. J.; Wiegreffe, P. W., to be submitted for publication.

(31) (a) English, A. D.; Herkovitz, T. *J. Am. Chem. Soc.* **1977**, *99*, 1648. (b) Behr, A.; Herdtweck, E.; Herrmann, W. A.; Keim, W.; Kipshagen, W. *J. Chem. Soc., Chem. Commun.* **1986**, 1262. (c) Tsuda, T.; Chujo, Y.; Saegusa, T. *J. Am. Chem. Soc.* **1978**, *100*, 630.

sterically more hindered. For example, although CO_2 insertion into the $(CO)_5Cr-OPh^-$ complex is faster than for the tungsten analogue, a reversal in the order of reactivity is noted as a function of the metal in the *cis*-$M(CO)_4(L)OPh^-$ anions (L = PMe_3, $P(OMe)_3$), i.e., W > Cr. Similarly, for *cis*-$W(CO)_4(L)OPh^-$ (L = CO, PMe_3, $P(OMe)_3$, and PPh_3), insertion of CO_2 or CS_2 indicates the following relative rate of insertion: CO ≫ $P(OMe)_3$ > PMe_3 > PPh_3, which parallels an increase in the L ligand's cone angle.[32] This observation is in contrast to the rate of CO_2 insertion into the W–CH_3 bond of *cis*-$CH_3W(CO)_4L^-$, where $P(OMe)_3$ and PMe_3 enhances the rate of CO_2 insertion over the all-carbonyl derivative.[27]

The addition of small quantities of water to THF solutions of the tungsten phenyl carbonate complexes lead to precipitation of bright-orange (CO_2 product) or dark brown (COS, CS_2 products) solid materials (eq 10–12). These materials are soluble in the

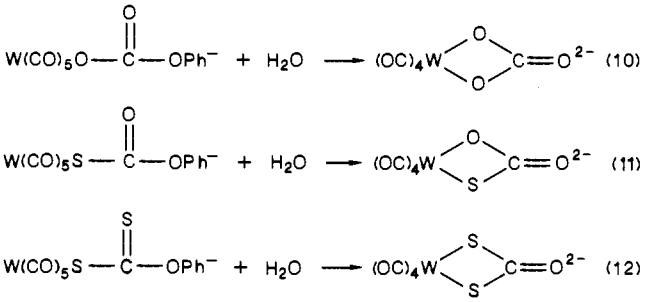

more polar solvents, acetone and acetonitrile, and have been spectroscopically characterized in these solvents by IR and ^{13}C NMR spectroscopies. The infrared spectral data exhibit ν(CO) band patterns typical of cis-disubstituted metal tetracarbonyl complexes, and the ^{13}C NMR spectra show 1:1 intensity ratios for the cis and trans carbonyl groups. The resonances for the carbonate carbons are very similar to those of the corresponding metal pentacarbonyl phenyl carbonates: WO_2COPh = 159.8 ppm vs WCO_3 = 161.1 ppm; WS_2COPh = 198.1 ppm vs WS_2CO = 200.0 ppm.

The mechanism proposed for carbonate formation involves primary attack of water at the electropositive carbonate carbon center generating a transient species. Loss of phenol from this species forms a tungsten bicarbonate complex, which is deprotonated with phenoxide or hydroxide prior or subsequent to CO loss and chelate formation. Consistent with the need for an added base, the yields of carbonate complexes are less than 50%. Other side products include $W(CO)_6$, $[W_4(CO)_{12}(OPh)_4]^{4-}$, and $W_2(CO)_{10}H^-$. Reactions of water with alkyl carbonates have been previously shown to convert these species to the corresponding metal bicarbonate complexes in certain copper[33,34] and palladium[35] systems.

X-ray-quality crystals of the product that results from hydrolysis of phenylcarbonate tungsten pentacarbonyl, $[Et_4N]_2[W(CO)_4(CO_3)\cdot H_2O]$, were grown from a wet acetone/diethyl ether solution. Tables VII and VIII contain the bond lengths and angles, respectively. The molecule as it occurs in the unit cell and the atomic-labeling scheme are shown in Figure 6. Two Et_4N^+ cations are oriented independently of the dianion. The four carbonyl groups are all bent away from the carbonate ligand, distorting the overall octahedral geometry about the tungsten center. The tungsten carbon bonds trans to the carbonate oxygen atoms (1.935 [6] Å) are shorter than the tungsten–carbon bonds cis to the carbonate ligand (2.016 [6] Å). The average W–O bond distance is 2.204 [4] Å). One water molecule crystallizes per complex. The hydrogen atoms were not located with precision. The oxygen–oxygen distance of 2.834 Å indicates only weak hydrogen bonding is present.

(32) Tolman, C. A. *Chem. Rev.* **1977**, *77*, 313.
(33) Tsuda, T.; Chujo, Y.; Saegusa, T. *J. Am. Chem. Soc.* **1980**, *102*, 431.
(34) Yamamoto, T.; Kubota, M.; Yamamoto, A. *Bull. Chem. Soc. Jpn.* **1980**, *53*, 680.
(35) Immirizi, A.; Musco, A. *Inorg. Chim. Acta* **1977**, *22*, L35.

Table VII. Bond Distances (angstroms) for $[Et_4N]_2[W(CO)_4CO_3]\cdot H_2O$

W–O(5)	2.203 (4)	W–O(6)	2.204 (4)
W–C(1)	1.935 (6)	W–C(2)	2.015 (6)
W–C(3)	1.935 (5)	W–C(4)	2.017 (6)
O(1)–C(1)	1.176 (8)	O(2)–C(2)	1.154 (9)
O(3)–C(3)	1.183 (7)	O(4)–C(4)	1.136 (8)
O(5)–C(22)	1.301 (6)	O(6)–C(22)	1.310 (7)
O(7)–C(22)	1.240 (7)	O(8)–Ho(8A)	0.838 (52)
O(8)–Ho(8B)	0.701 (68)	Ho(8A)–Ho(8B)	1.134 (84)
O(7)–O(8)	2.834	N(1)–C(6)	1.533 (7)
N(1)–C(8)	1.521 (7)	N(1)–C(10)	1.510 (8)
N(1)–C(12)	1.531 (8)	N(2)–C(14)	1.514 (9)
N(2)–C(16)	1.520 (8)	N(2)–C(18)	1.511 (8)
N(2)–C(20)	1.520 (7)	C(6)–H(6A)	0.976 (42)
C(6)–H(6B)	1.062 (64)	C(6)–C(7)	1.498 (9)
C(7)–H(7A)	0.984 (85)	C(7)–H(7B)	0.903 (76)
C(7)–H(7C)	0.919 (56)	C(8)–H(8A)	1.026 (66)
C(8)–H(8B)	1.079 (58)	C(8)–C(9)	1.493 (10)
C(9)–H(9A)	0.925 (64)	C(9)–H(9B)	0.961 (65)
C(9)–H(9C)	0.917 (68)	C(10)–H(10A)	1.006 (78)
C(10)–H(10B)	1.114 (60)	C(10)–C(11)	1.491 (9)
C(11)–H(11A)	1.002 (62)	C(11)–H(11B)	1.051 (87)
C(11)–H(11C)	0.825 (77)	C(12)–H(12A)	1.077 (51)
C(12)–H(12B)	0.940 (37)	C(12)–C(13)	1.501 (10)
C(13)–H(13A)	0.847 (94)	C(13)–H(13B)	0.949 (96)
C(13)–H(13C)	0.889 (72)	C(14)–H(14A)	1.016 (73)
C(14)–H(14B)	0.943 (66)	C(14)–C(15)	1.492 (10)
C(15)–H(15A)	0.977 (57)	C(15)–H(15B)	1.017 (72)
C(15)–H(15C)	0.937 (80)	C(16)–H(16A)	1.022 (62)
C(16)–H(16B)	1.039 (56)	C(16)–C(17)	1.510 (13)
C(17)–H(17A)	1.037 (80)	C(17)–H(17B)	0.920 (63)
C(17)–H(17C)	0.885 (77)	C(18)–H(18A)	0.987 (52)
C(18)–H(18B)	0.888 (46)	C(18)–C(19)	1.510 (9)
C(19)–H(19A)	0.881 (59)	C(19)–H(19B)	0.823 (77)
C(19)–H(19C)	1.046 (78)	C(20)–H(20A)	0.945 (63)
C(20)–H(20B)	0.919 (53)	C(20)–C(21)	1.494 (12)
C(21)–H(21A)	0.958 (51)	C(21)–H(21B)	1.153 (66)
C(21)–H(21C)	0.992 (86)		

Table VIII. Bond Angles (degrees) for $[Et_4N]_2[W(CO)_4CO_3\cdot H_2O]$

O(5)–W–O(6)	59.4 (1)	O(5)–W–C(1)	165.9 (2)
O(6)–W–C(1)	106.6 (2)	O(5)–W–C(2)	96.9 (2)
O(6)–W–C(2)	97.1 (2)	C(1)–W–C(2)	81.9 (2)
O(5)–W–C(13)	106.1 (2)	O(6)–W–C(3)	165.3 (2)
C(1)–W–C(3)	87.9 (2)	C(2)–W–C(3)	86.7 (2)
O(5)–W–C(4)	96.2 (2)	O(6)–W–C(4)	94.6 (2)
C(1)–W–C(4)	86.9 (2)	C(2)–W–C(4)	165.7 (3)
C(3)–W–C(4)	84.0 (3)	W–O(5)–C(22)	93.6 (3)
W–O(6)–C(22)	93.3 (3)	Ho(8A)–O(8)–Ho(8B)	94.5 (69)
C(6)–N(1)–C(8)	110.9 (4)	C(6)–N(1)–C(10)	108.5 (4)
C(8)–N(1)–C(10)	110.0 (4)	C(6)–N(1)–C(12)	108.2 (4)
C(8)–N(1)–C(12)	107.3 (4)	C(10)–N(1)–C(12)	111.9 (4)
C(14)–N(2)–C(16)	111.2 (5)	C(14)–N(2)–C(18)	111.2 (5)
C(16)–N(2)–C(18)	105.2 (5)	C(14)–N(2)–C(20)	106.5 (5)
C(16)–N(2)–C(20)	111.4 (5)	C(18)–N(1)–C(20)	111.4 (5)
W–C(1)–O(1)	178.2 (5)	W–C(2)–O(2)	169.3 (6)
W–C(3)–O(3)	178.7 (5)	W–C(4)–O(4)	170.1 (6)
N(1)–C(6)–C(7)	115.8 (5)	N(1)–C(8)–C(9)	115.5 (5)
N(1)–C(10)–C(11)	115.7 (6)	N(1)–C(12)–C(13)	115.3 (6)
N(2)–C(14)–C(15)	115.7 (6)	N(2)–C(16)–C(17)	114.3 (7)
N(2)–C(18)–C(19)	115.1 (6)	N(2)–C(20)–C(21)	116.2 (6)
O(5)–C(22)–O(6)	113.7 (5)	O(5)–C(22)–O(7)	124.2 (5)
O(6)–C(22)–O(7)	122.1 (5)		

The tungsten–oxygen distances of 2.203 and 2.204 Å are similar to the tungsten–oxygen distances in the two anions of $[Et_4N][W(CO)_5OPh]$, 2.181 and 2.203 Å. The angles within the dianion show the carbonyl ligands trans to the carbonate are bent away from the carbonate moiety: O(6)–WC(1) is 106.6°; O(5)–W–C(3) is 106.1°. The C(1)–W–C(3) angle is nearly 90°, at 87.9°. However, the O(5)–W–O(6) angle of the tungsten atom to the carbonate oxygens is very acute, 59.4°.

This molecule is very interesting in that it possesses carbon–oxygen single, double, and triple bonds. The C(22)–O(5) and C(22)–O(6) bond length are 1.310 and 1.301 Å, carbon–oxygen single bonds. The C(22)–O(7) bond length is 1.240 Å, a car-

bon-oxygen double bond. The carbonyl ligands possess carbon-oxygen triple bonds with an average value of 1.16 Å.

Acknowledgment. Financial support of this research by the National Science Foundation (Grant CHE 88-17873) and the Robert A. Welch Foundation is greatly appreciated.

Registry No. I, 106162-73-6; II, 121918-96-5; III, 106162-80-5; [PPN][OPh], 121888-64-0; $[Et_4N][OPh]$, 32580-85-1; $[Et_4N][OC_6H_4CH_3$-*m*], 121888-65-1; $[Et_4N][Cr(CO)_5OPh]$, 121918-63-6; $Cr(CO)_6$, 13007-92-6; $Cr(CO)_5THF$, 15038-41-2; $[Et_4N][Cr(CO)_5COOPh]$, 121918-65-8; $[Et_4N][Cr_4(CO)_{12}(OPh)_4]$, 97879-19-1; $W(CO)_5THF$, 36477-75-5; $W(CO)_6$, 14040-11-0; $[Et_4N][W(^{13}CO)_5OPh]$, 121918-67-0; $[PPN][W(CO)_5OPh]$, 121918-68-1; $[Et_4N][W(CO)_5COOPh]$, 121918-69-2; $[Et_4N][W_4(CO)_{12}(OPh)_4]$, 106191-48-4; $[Et_4N][cis$-$Cr(CO)_4(PMe_3)OPh]$, 121918-71-6; $[Et_4N][cis$-$Cr(CO)_4(P(OMe)_3)OPh]$, 121918-73-8; $[Et_4N][cis$-$W(CO)_4(PMe_3)OPh]$, 121918-75-0; $[Et_4N][cis$-$W(CO)_4(P(OMe)_3)OPh]$, 121918-77-2; $[Et_4N][cis$-$W(CO)_4(PPh_3)OPh]$, 121918-79-4; $[Et_4N][Cr(CO)_5O_2COPh]$, 121918-81-8; $[Et_4N][Cr(CO)_5SC(O)OPh]$, 121918-83-0; $[Et_4N[[Cr(CO)_5S_2COPh]$, 121918-85-2; $[Et_4N][W(CO)_5O_2COPh]$, 121918-86-3; $[Et_4N][W(CO)_5O_2COC_6H_4CH_3$-*m*], 121918-87-4; $[Et_4N][W(CO)_5OC_6H_4CH_3$-*m*], 106162-75-8; $[Et_4N][W(CO)_5SC(O)OPh]$, 121918-89-6; $[Et_4N][W(CO)_5S_2COPh]$, 121918-91-0; $[Et_4N]_2[W(CO)_4CO_3]$, 106162-79-2; $[Et_4N]_2[W(CO)_4(CO_2S)]$, 121918-93-2; $[Et_4N]_2[W(CO)_4S_2CO]$, 121918-95-4; CO_2, 124-38-9; COS, 463-58-1; CS_2, 75-15-0; phenol, 108-95-2.

Supplementary Material Available: Drawing with the labeling scheme for the $[Et_4N]^+$ cations in $[Et_4N][W(CO)_5OPh\cdot0.5H_2O]$ (II, Figure 1S), figure of the unit cell of $[Et_4N][W(CO)_5OPh]$ (Figure 2S), figure of the unit cell of $[Et_4N][W(CO)_5OPh\cdot0.5H_2O]$ (Figure 3S), table of infrared spectral data for the complexes $[Et_4N][M(CO)_5OR]$ in THF (Table 1S), tables of atomic coordinates for $[Et_4N][W(CO)_5OPh]$ (I, Table 2S), $[Et_4N][W(CO)_5OPh\cdot0.5H_2O]$ (II, Table 3S), and $[Et_4N]_2[W(CO)_3\cdot H_2O]$ (III, Table 4S), tables of anisotropic thermal parameters for I (Table 5S), II (Table 6S), and III (Table 7S), H atom coordinates and isotropic thermal parameters of I (Table 8S), II (Table 9S), and III (Table 10S) (12 pages); listing of calculated and observed structure factor amplitudes for I (Table 11S), II (Table 12S), and III (Table 13S) (55 pages). Ordering information is given on any current masthead page.

X-ray Absorption Edge and EXAFS Study of the Copper Sites in ZnO Methanol Synthesis Catalysts

Lung-Shan Kau, Keith O. Hodgson,* and Edward I. Solomon*

Contribution from the Department of Chemistry, Stanford University, Stanford, California 94305. *Received August 15, 1988*

Abstract: X-ray absorption edge and EXAFS data are presented for the binary form of the Cu-ZnO methanol synthesis catalysts. For the calcined catalyst, a significant amount of the Cu(II) is found to be doped into the tetrahedral sites of the ZnO lattice based on a quantitative analysis of X-ray absorption difference edges. Alternatively, the EXAFS spectra exhibit less evidence for this Cu(II)/ZnO site, which is attributed to disorder effects on the outer-shell Cu-Zn EXAFS. A quantitative analysis of the EXAFS for the reduced catalyst demonstrates that it contains metallic Cu, small Cu clusters, and a Cu oxide phase. Analysis of the X-ray absorption edges of the reduced catalyst shows that this oxide phase contains both Cu_2O and tetrahedral Cu(I) sites. Thus, the dispersed phase in the methanol synthesis catalyst, which corresponds to ~50% of the Cu, consists of both a small Cu cluster component and Cu(I) doped into the ZnO lattice.

ZnO is an effective catalyst for the hydrogenation of CO to CH_3OH. The active high-temperature, high-pressure catalyst also contains either Al_2O_3 or Cr_2O_3, which acts as an intercrystalline promoter to inhibit sintering of ZnO crystallites,[1] with ZnO being the active phase. The chemisorption properties of CO on the four chemically different, low index surfaces of ZnO have been defined in detail by using angle-resolved photoelectron and high-resolution electron energy loss spectroscopies.[2] These studies show that CO binds carbon end down to the coordinatively unsaturated Zn(II) on terrace and step sites, depending on the surface.

The catalytic activity of ZnO for methanol synthesis can be strongly enhanced by the addition of a small amount of Cu. Binary Cu/ZnO is a low-temperature, low-pressure catalyst[3] which is obtained by reduction of CuO/ZnO. The maximum rate of methanol synthesis appears at catalyst compositions near a CuO:ZnO ratio of 30:70. The Cu component is thought to act as an intracrystalline promoter that significantly lowers the activation barrier for the reaction (from ~30 to 18 kcal/mol).[4] The presence of a small amount of CO_2 in the feed gas is required to prevent catalyst deactivation. While there have been a number of investigations of the mechanism of methanol synthesis on the Cu/ZnO heterogeneous catalyst and of the CO_2 promotion effect, these are still not well understood.

Recent studies have demonstrated that the reduced catalyst contains, in addition to the ZnO and metallic Cu, a significant amount of the Cu in a dispersed phase. Using a combination of techniques (X-ray photoelectron spectroscopy (XPS), Auger, scanning transmission electron microscopy and surface area measurements), Klier et al.[5] concluded for the activated catalyst

(1) (a) Natta, G. *Catalysis* **1955**, *3*, 349. (b) Burzyk, J.; Haber, J. *Bull. Acad. Pol. Sci. Ser. Sci. Chim.* **1969**, *17*, 531. (c) *Ibid.* 539. (d) Burzyk, J.; Haber, J.; Nowotny, J. *Ibid.* 543.

(2) (a) D'Amico, K. L.; McFeely, F. R.; Solomon, E. I. *J. Am. Chem. Soc.* **1983**, *105*, 6380. (b) D'Amico, K. L.; Trenary, M.; Shinn, N. D.; Solomon, E. I.; McFeely, F. R. *J. Am. Chem. Soc.* **1982**, *104*, 5102. (c) Gay, R. R.; Nodine, M. H.; Henrich, V. E.; Zeiger, H. J.; Solomon, E. I. *J. Am. Chem. Soc.* **1980**, *102*, 6752.

(3) Klier, K. *Adv. Catal.* **1982**, *31*, 243, and references therein.

(4) Emmett, P. H. In *Catalysis Then and Now*; Emmett, P. H., Sabbatier, P., Reid, E. E., Eds.; Franklin Publishing: Englewood, NJ, 1965; Part I, pp 173.

(5) (a) Parris, G. E. Ph.D. Thesis, Lehigh University, 1982. (b) Dominiquez, J. M.; Simmons, G. W.; Klier, K. *J. Mol. Catal.* **1983**, *20*, 369. (c) Klier, K.; Chatikavanij, V.; Herman, R. G. *J. Catal.* **1982**, *74*, 343. (d) Metha, S.; Simmons, G. W.; Klier, K.; Herman, R. G. *J. Catal.* **1979**, *57*, 339. (e) Bulko, J. B.; Simmons, G. W.; Klier, K.; Herman, R. G. *J. Phys. Chem.* **1979**, *83*, 3118. (f) Herman, R. G.; Klier, K.; Simmons, G. W.; Finn, B. P.; Bulko, J. B.; Kobylinske, T. P. *J. Catal.* **1979**, *56*, 407.

0002-7863/89/1511-7103$01.50/0